Summer 6-12-2019

The Mechanism KSHV Plays in Mesenchymal to Endothelial Transition in Kaposi Sarcoma

Sausan Alfaris
salfaris@upenn.edu

The Mechanism KSHV Plays in Mesenchymal to Endothelial Transition in Kaposi Sarcoma

Abstract
To gain a better understanding of the tumorigenesis of Kaposi sarcoma (KS) it is essential to understand the role KSHV plays in the mesenchymal-to endothelial transition (MEndT). PROX1 in human related cancers can act as a transcriptional repressor or activator that leads to several effects on cellular differentiation and proliferation[1-3]. PROX1 upregulation may play a significant role in the MEndT and in turn effect the tumorigenesis of KS. This study was conducted to evaluate if PROX1 is upregulated by KSHV. To test this, human GMSCs and human PDLSCs were used, as well as 293T cells. They were transfected at 70% confluency using Lipofectamine 3000 with a PROX1 promoter, pPROX1, cloned into a pGL3 promoter. The cells were then infected using recombinant green fluorescent protein (GFP) expressing KSHV (rKSHV.219) . A luciferase assay was conducted to measure expression of pPROX1. The samples were lysed and collected at different time points (24, 36, 48 hours). Results show that in 293Tcells KSHV infected cells do not exhibit noticeable luciferase signal activation of pPROX1 at 24, 36, and 48 hours post infection, PDLSCs show a slight increase in luciferase signal in KSHV+ pGL3-PROX1 v6 is at 24, 36 and 48 hours post infection, while in KSHV infected GMSCs do not exhibit noticeable luciferase signal activation of pPROX1 at 24,36 and 48 hours. In conclusion, there is no significant activation of pPROX1 in KSHV infected 293Tcells, PDLSCs, and GMSCs. Future experiments that are warranted would be assessing the upregulation of PROX1 via Western Blot and RT-PCR.

Degree Type
Thesis

Degree Name
MSOB (Master of Science in Oral Biology)

Subject Categories
Dentistry

University of Pennsylvania Dental Medicine

Thesis

The Mechanism KSHV plays in Mesenchymal to Endothelial Transition in Kaposi Sarcoma

Degree Name

MSOB (Master of Science in Oral Biology)

Primary Advisor

Claire Mitchell, PhD

A Thesis Presented to the Faculty of Penn Dental Medicine in Fulfillment of the Requirements for the Degree of Master of Science in Oral Biology 2019

Thesis Committee:

Jonathan Korostoff, DMD,PhD Professor of Periodontics, Director, Master of Science in Oral Biology Program Department of Periodontics -Chair

Claire Mitchell, PhD Professor Department of Anatomy and Cell Biology

Yan Yuan, PhD. Professor. Department of Microbiology

Mel Mupparapu DMD, Professor of Oral Medicine and Director of Radiology at Penn Dental Medicine, Program Director of the Oral & Maxillofacial Radiology Fellowship

TABLE OF CONTENTS

Acknowledgment:

I would like to thank Dr. Mitchell for giving me the opportunity to work under her supervision and guidance, and for her continuous support and encouragement. I would also like to thank the Mitchell and Yuan lab for their helpful assistance, constructive discussion and suggestions. Moreover, I would like to extend my deepest appreciation to my committee members for being gracious with their time and being part of my thesis committee.

I would like to thank my family for their unconditional love, support, and encouragement in every step of this journey.

Lastly, I would like to thank my friends for all the support and patience that they have given me, and for all the long nights they stayed with me and for all the moments I wanted to give up but wouldn't let me. Thank you!

;

Abstract:

To gain a better understanding of the tumorigenesis of Kaposi sarcoma (KS) it is essential to understand the role KSHV plays in the mesenchymal-to endothelial transition (MEndT). PROX1 in human related cancers can act as a transcriptional repressor or activator that leads to several effects on cellular differentiation and proliferation[1-3]. PROX1 upregulation may play a significant role in the MEndT and in turn effect the tumorigenesis of KS. This study was conducted to evaluate if PROX1 is upregulated by KSHV. To test this, human GMSCs and human PDLSCs were used, as well as 293T cells. They were transfected at 70% confluency using Lipofectamine 3000 with a PROX1 promoter, pPROX1, cloned into a pGL3 promoter. The cells were then infected using recombinant green fluorescent protein (GFP) expressing KSHV (rKSHV.219) . A luciferase assay was conducted to measure expression of pPROX1. The samples were lysed and collected at different time points (24, 36, 48 hours). Results show that in 293Tcells KSHV infected cells do not exhibit noticeable luciferase signal activation of pPROX1 at 24, 36, and 48 hours post infection, PDLSCs show a slight increase in luciferase signal in KSHV+ pGL3-PROX1 v6 is at 24, 36 and 48 hours post infection, while in KSHV infected GMSCs do not exhibit noticeable luciferase signal activation of pPROX1 at 24,36 and 48 hours. In conclusion, there is no significant activation of pPROX1 in KSHV infected 293Tcells, PDLSCs, and GMSCs. Future experiments that are warranted would be assessing the upregulation of PROX1 via Western Blot and RT-PCR.

Introduction:

Kaposi sarcoma, KS, is considered a vascular neoplasm. It can be used as a model to study many aspects of carcinogenesis including cancer immunology, viral oncogenesis and angiogenesis. KS can involve the mucosa, skin, and viscera [4,5]. Kaposi's sarcoma-associated herpesvirus, KSHV, encodes several genes that target cellular oncogenic, survival and tumor suppressor genes, but the mechanism remains unclear [6]. Tumor cells infected with KSHV manifest the classic spindle shape morphology, expressing lymphatic endothelial, vascular endothelial and mesenchymal markers[7 8].

Immunohistochemical features of KS include mesenchymal and precursor markers, which suggest that KS could originate from pluripotent mesenchymal stem cells, MSCs. KS has been shown to confer MSCs with KS associated phenotypes such as angiogenesis, endothelial cell linage and cytokine/chemokine production [9 3]. There is a need to better understand how KSHV infection reprograms infected MSCs by activating numerous genes to start the mesenchymal to endothelial transition, MEndT. KSHV affects the expression of several linage specific genes. In MSCs, MEndT related genes (PDPN, EDNRA, and PML D106) were found to be upregulated in response to KSHV infection. PROX1 in human related cancers can act as a transcriptional repressor or activator that leads to several effects on cellular differentiation and proliferation. PROX1 upregulation might play a significant role in the tumorigenesis of KS and further studies are warranted to evaluate its role.

Cellular origin of Kaposi sarcoma:

Despite many studies that have been done to establish the cellular origin of KS, the origin of KS cells remain a mystery. Tumor cells infected with KSHV manifest the classic spindle shape morphology, expressing lymphatic endothelial, vascular endothelial and mesenchymal markers[7]. Studies supporting the theory that KS is of endothelial cell linage argue that evidence indicate the lymphatic origin. KSHV-infected ECs display increased proliferative, angiogenic and migratory capacities which account for KS oncogenesis. Different studies have reported that sarcoma cells express a number of endothelial cell, EC, markers. For example, CD31, CD34, and FACTORVIII are expressed in both SC and EC lines, but they also express lineage specific signatures of smooth muscle cells, α-SMA), monocytes, macrophages, dendritic cells, fibroblasts and mesenchymal cells[4,10].

The gene expression signature of KSHV infected cells might indicate an endothelial origin, but it is still a matter of debate whether the original precursor belongs to blood or lymphatic lineage. KSHV infected lymphatic ECs, LEC's, or KSHV-LECs are more similar to immature blood ECs, BECs, than uninfected LECs by the virus triggering cellular reprogramming towards a more pluripotent state. KSHV-infected BECs however, express lower levels of blood vascular markers, like Cxcr4 and Neuropilin-1 show an increase in lymphatic markers like Prox1, Vegfr3, Podaplanin and Lyve1. KSHV infection of ECs reverses the differentiated EC fate and recovers the pluripotent, even mesenchymal stem-cell lineage with mixed identity. As a result, KSHV-infected ECs display tumorigenic properties, i.e. increased angiogenic, invasive and migratory

abilities, and while not fully immortalized, they exhibit a growth advantage over their uninfected counterparts [11].

Several observations suggest that LECs, rather than BECs, are the main precursor of SCs. First, the localization of KS lesions in tissues rich in lymphatics (skin and mucosa). Secondly, cultured KSHV-LECs exhibit elongated (spindle) morphology, resembling KS-SCs, whereas in BECs the morphology is not significantly altered by KSHV infection. Furthermore, LECs can be more efficiently infected and harbor a higher viral copy number. The comparison of the gene expression profile of nodular KS lesion with those of BECs and LECs showed that the KS signature resembles more like LECs rather than BECs. Moreover, three-dimensional cultures of KSHV-LECs, has been shown to recapitulate many of the features found in the KS lesions. The differential expression of endothelial and mesenchymal markers in virus-infected cells and the tumorigenic invasiveness increases in the 3D matrix[11,12].

Regardless, the presence of KSHV-infected BECs in KS lesions cannot be ruled out. KSHV-BECs are found in early KS patches, whereas KSHV-positive cells line aberrant blood vessels. While the advanced lesions does represent the majority of the tumor mass, KSHV-SCs were not found in blood vessels. One could hypothesize that KSHV infects both BEC and LEC at the early stages of the disease, but then KSHV-LECs are more susceptible hosts for the virus, propagate more efficiently, and become the predominant cell type in the advanced lesion. In agreement with this hypothesis, a study in which PROX1 expression, a marker of lymphatic differentiation, was investigated in

AIDS-oral KS. Here, PROX1, almost absent in early KS patches, increased significantly in advanced plaque and nodular stages. Another possibility is that KS-SCs originate from the infection of circulating EC precursors (ECPs), CD34-positive bone marrow-derived cells that aggregate to angiogenic sites where they then differentiate into mature ECs. In support for this hypothesis, ECPs isolated from KS patients were found positive for KSHV, retained the virus after several passages, and were able to sustain lytic replication. Also, ECPs from KS patients displayed higher angiogenic potential *in vitro*, KSHV-positive, CD34+, adherent SCs were found in the blood mononuclear fraction, and finally the multifocal nature of KS lesions occur independently in different areas of the body, preferentially in surgical scar sites and other sites of previous inflammation angiogenesis, which are areas where ECPs are recruited[5,13]. Recent emerging studies now support the theory that the transition could be mesenchymal to endothelial. Immunohistochemical features of KS include mesenchymal and precursor markers, which suggest that KS could originate from pluripotent mesenchymal stem cells, MSCs. A study conducted by Yuan et al. has shown that KS can confer MSCs with KS associated phenotypes such as angiogenesis, endothelial cell linage, and cytokine/chemokine production[9]. There is a need to better understand how KSHV infection reprograms infected MSCs by activating numerous genes to start the mesenchymal to endothelial transition (MEndT). KSHV affects the expression of several linage specific genes. In MSCs (MEndT) related genes (PROX1, PDPN, EDNRA, PML, PGF, and TGF-b3) were found to be upregulated in response to KSHV infection while in KSHV infected LECs PROX1 was found to be down regulated and no change was

noted in the levels of (PDPN, EDNRA, PML, PGF, and TGF-b3). PROX1 upregulation triggers the tumorigenesis of KS[14-16]**.**

The role of PROX1:

The Prospero Homeobox 1 gene PROX1 is the vertebrate homologue of *Drosophila* prospero gene. It is a transcription factor that plays an important role in the development of the liver, central nervous system, pancreas and in lens fiber elongation. It is a master regulator that influences the healthy embryonic development of lymphatic vasculature [17] [18] [19]. The role PROX1 plays in Kaposi sarcoma and cell differentiation is still poorly understood. A review conducted by Cancian et al. stated that the up regulation of PROX1 in KSHV infected BECs switches on LEC-specific genes in the blood vasculature [8]. If PROX1 is silenced during the infection of BECs this inhibits KSHV-mediated upregulation of many key lymphatic genes, demonstrating that PROX1 is important for KSHV driven BEC-to-LEC reprogramming[8]. The expression of PROX1 is one of the first indications that the molecular program leading to lymphatic vasculature formation is starting. This primary expression followed by migration of PROX1-expressing endothelial lymphatic progenitor endothelial cells that gradually increase the expression of lymphatic markers like VEGFR-3 and down regulates the expression of blood vascular genes like Lamninin and CD34. This confirms the important role of PROX1 is established by stimulating undifferentiated endothelial cells to commit to a lymphatic fate[1,17,20].

Studies have shown that the lymphatic and blood vasculature are greatly similar since both are lined with endothelial cells and share some markers. Furthermore, the expression of additional gene products might be enough to convert endothelial cells if required to blood vascular phenotype into a lymphatic phenotype. Through this, PROX1 has been determined as a master regulator of the molecular switch, since its expression is enough to override the blood vasculature phenotype in primary human endothelial cells by promoting a lymphatic endothelial phenotype instead[18,21]. It is thought that PROX1 plays an essential role as a switch necessary to promote and maintain lymphatic endothelial cell identity and suppress blood vascular endothelial cell identity. Variations in the levels of PROX1 expression are triggers to differentiate lymphatic endothelial cell phenotype into a blood vascular endothelial cell phenotype, which verifies that PROX1 activity is required not only for cell type specification but also to preserve the mature differentiated lymphatic endothelial cell phenotype. Moreover, the lymphatic endothelial cell phenotype is lost when PROX1 is expressed below a certain threshold. In embryonic and mature lymphatic vasculature, constant PROX1 expression is necessary to maintain the lymphatic endothelial cell identity and suppression of default blood vascular endothelial cell identity[13,18]. PROX1 could act as a master switch in this process and the study of cellular reprograming and plasticity as well as gene modulation would help to better understand this mechanism[14,17,22,23].

Study design :

Study Objective: The objective of this study is to understand the potential effects that KSHV has on specific gene expression and the invasive and aggressive nature of the biology of KS in vivo.

Hypothesis:

- PROX1 could be expressed at higher levels in KSHV infected gingival mesenchymal cells (GMSC) and periodontal mesenchymal cells (PDLSC), in comparison to uninfected GMSCs and PDLSCs.
- KSHV infection could increases expression of PROX1 in GMSC and PDLSC. This will be tested using a luciferase assay on both mesenchymal and 293T cells.

Significance:

Grasp an understanding of the function of PROX1. The pathological role PROX1 plays in KS is poorly understood, could lymphatic reprograming be a goal of PROX1 upregulation or a byproduct in Kaposi sarcoma? Many studies have shown that PROX1 in some cancers is oncogenic and in others plays a tumor suppressive [22]. Therefore, the tissue microenvironment and cell type may be important for PROX1 to be oncogenic or tumor suppressive [24]. The proposed project will help to understand the key role PROX1 plays in KS.

Significant impact on the understanding of Kaposi sarcoma (KS). KS is undeniably the most common malignancy HIV patients suffer from. It is characterized by abnormal

inflammation neoagniogensis and proliferation of spindle cells [4,5]. Examining the cellular origin of KS and the method in which the tumor affects the normal differential pathways through specific transcriptional factors like PROX1 is crucial to understanding the diseases progression[17]. The proposed project will shed light on the progression of Kaposi sarcoma.

Design for new treatments and therapies. The method in which PROX1 affects essential pathways in tumorigenesis is not well comprehended[22]. The aim of this project is to shed light on the underlying mechanisms affected by PROX1 in Kaposi sarcoma which could contribute to the development of new therapies and treatments.

Chapter 2

Materials and methods:

RNA-Seq data analysis. RNA-seq data was aligned against human (GRCh38.p12) genome and transcriptomes using Hisat2 algorithm. Raw counts were converted to log2 (5+count) values and quantile normalized to use in Principle Component Analysis and gene expression heatmaps. Significance and fold change of differential expression between lesion and control samples was estimated using the DESeq2 method on raw values and genes with false discovery rate (FDR) <5% were considered as significant. An additional threshold of 5-fold was used to enumerate a set of most-changed genes between conditions. Pearson correlation was used to test associations between KSHV transcript loads in cultures for significantly differentially expressed genes. Correlations with $p<0.05$ were considered significant. Expression heatmaps were plotted in Microsoft Excel using normalized values centered versus average across all samples. Differentially expressed genes were then used for GeneOnotology analysis using Panther14.1 classification system.

Culturing of iSLK-BAC16 cells and Virus Purification. iSLK-BAC16 cells were seeded at 2.1 x 10^6 cells/flask of a T75 flask or ~70% confluence. iSLK-BAC16 cells were cultured in Dulbecco's modified Eagle's medium (DMEM) that was supplemented with 10% fetal bovine serum and in the presence of 1 µg/ml puromycin, 250 µg/ml G418, and 1,200 µg/ml hygromycin B. Cells were incubated at 37°C with a humidified atmosphere of 5% CO2.

iSLK-BAC16 cells were induced in the presence of both doxycycline (1 μg/ml) and sodium butyrate (1 mM) and the absence of hygromycin, puromycin, and G418. Four days later, supernatant was collected and cleared of cells and debris by centrifugation (950xg for 10 minutes at 4°C) and filtered (0.45 μm). Virus particles were pelleted by ultracentrifugation (25,000 g for 3 hours at 4°C) with a 5mL 25% sucrose cushion using an SW32 Ti rotor. Pellets were resuspended in 200uL of 1xPBS and frozen at -80°C for long term storage.

Quantification of Virions. Following pelleting of virion particles, to remove contaminating DNA outside viral particles, the concentrated viruses were treated with Turbo DNase I (Ambion) at 37°C for 1 h, followed by proteinase K digestion. Virion DNA was extracted with phenol-chloroform, precipitated with ice-cold ethanol, and then dissolved in Tris-EDTA (TE) buffer. The KSHV genomic copy number was quantified by real-time PCR using SYBR green kit with primers for the detection of LANA (forward, 5′-CGCGAATACCGCTATGTACTCA-3′; reverse, 5′-GGAACGCGCCTCATACGA-3′). Viron samples were loaded onto a MicroAmp Optical 96-well reaction plate in an increasing 10-fold serial dilution. CT values were compared to a known LANA standard that was isolated through plasmid digest and gel isolation to isolate the LANA fragment following agarose gel electrophoresis.

Promoter Identification. Ensembl database using GRCh38.p12 (Genome Reference Consortium Human Build 38), INSDC Assembly GCA_000001405.27, Dec 2013 was

used to identify the promoter and promoter flanking region coordinates, ENSR00000386083. Promoter sequence was then determined using NCBI FASTA viewer.

Isolation of Human Genomic DNA from 293T cells. 293T cells were cultured were cultured in DMEM supplemented with 10% fetal bovine serum with 100U/mL penicillin/streptomycin antibiotic solution and harvested by using 0.05% (w/v) Trypsin in 0.53 mM EDTA solution. DNA was isolated using QIAamp DNA Mini Kit (Qiagen) following the provided kit protocol.

Cloning PROX1 Promoter Region. Primers used to amplify the PROX1 promoter region from human genomic DNA were designed to have a four nucleotide non-homologous nonsense overhang (CCCC or GCGC) followed by NheI digest site for the forward primer and HindIII digest site for the reverse primer. pPROX1 version 6 primers (forward, 5'- CCCCGCTAGCATTTGGACTGGAGATAAACTGGGA-3' and reverse, 5'-GGGGAAGCTTAGGTACCACCCAGACGAGA-3'). Version 7 primers (forward, 5'-GCGCGCGCTAGCCCAGATGTTTGCAACATATA-3' and reverse, 5'-GCGCGCAAGCTTGCAGGAGAAAGAAGGAAAGG-3'). PCR amplification was done using GoTaq Green Master Mix (Promega) and conducted using the provided manufacturer's protocol.

Phenol-Chloroform Extraction. The PCR product of pPROX1, either version 6 or version 7, was separately pooled to a total volume of 500uL each. One equal volume of

phenol:chloroform:isoamyl alcohol (25:24:1) was added to each sample and vortexed for 20 seconds. Phase separation was done by centrifugation at room temperature for 15 minutes at 16,000g. The aqueous phase was transferred to a clean Eppendorf tube and solution was brought to 3M Ammonium acetate (NH4OAc) and brought to 1.2mL using 100% isopropanol. Samples were incubated at -20°C overnight to precipitate the DNA from the samples. Samples were centrifuged at 4°C for 30 minutes at 16,000g to pellet the cDNA. Pellets were washed by in 70% ethanol. Pellets were air dried and resuspended in 30uL of 1xTE buffer. DNA concentrations were then quantified on NanoDrop.

Restriction Enzyme Digestion. Purified PCR pPROX1 samples and PGL3 were then subjected to NheI and HindIII double restriction enzyme digest. Reaction was set up according to recommended New England Biolabs (NEB) protocol using Restriction Enzyme Buffer 2 (50 mM NaCl, 10 mM Tris-HCl, 10 mM, MgCl2, 1 mM DTT final concentration). The final concentration of glycerol in the digest reaction was less than 5% to minimize the possibility of star activity. Reaction was done for 1hr at 37C, PCR pPROX1 products were then purified using phenol-chloroform extraction as described previously. PGL3 plasmid was then loaded onto a 1% agarose gel for gel band extraction.

Gel Electrophoresis and Gel Band Extraction. A 100mL 1% melted agarose gel in 1x tris-acetate-EDTA (1x TAE) was prepared with ethidium bromide (EtBr) to a final concentration of approximately 0.5 µg/mL. Samples and standard gel ladder was loaded

and run at 100 volts for 1 hour. Digested PGL3 gel band (4818bp) was identified under UV light and excised using a sterile scalpel. Gel fragment containing desired DNA product was then used in QIAquick Gel Extraction Kit following provided manufacturer's protocol (Qiagen).

T4 Ligation. Purified digested plasmid and promoters were ligated following manufacturer's provided protocol (NEB) for cohesive sticky end ligation using a molar ratio of 1:3 vector to insert. Reactions were incubated at 16°C overnight, then heat inactivated at 65°C for 10 minutes. Samples were chilled on ice and 2µl of the reaction was transformed into 50 µl of competent cells.

Preparing Competent Cells for Transformation. The Escherichia XL1-Blue strain genotype: recA1 endA1 gyrA96 thi-1 hsdR17 supE44 relA1 lac [F′ proAB lacIq ZΔM15 Tn10 (Tetr)]. Bacterial strain was streaked from frozen glycerol stock on Luria-Bertani, LB, plates and incubated at 37°C overnight. Individual colony was picked and cultured in 2mL liquid LB media and incubated at 37°C overnight under constant agitation. 1mL of inoculate was used to culture 100mL LB and incubated at 37°C under constant agitation for ~2 hours until torrid OD600=0.25-0.4. Culture was chilled on ice for 15 minutes and centrifuged at 3000g for 10 minutes at 4C. Pellet was resuspended in 40mL ice cold 0.1M CaCl2. Pellet was resuspended in 8mL of 0.1M CaCl2 Solution plus 15% Glycerol. Cells were aliquoted and flash frozen in liquid nitrogen prior to long term storage at -80C.

Luria-Bertani ampicillin culture plates. 15 g of Bacto-agar was dissolved in 1.0 L of LB medium and sterilize by autoclaving. Solution was cooled to 50°C in a temperature-controlled water bath and 0.50 mL of 100 mg/mL ampicillin was added prior to pouring into plates.

Transformation and Screening. Competent cells were thawed on ice, 50µl of competent cells were added to DNA solution and gently mixed. Mixture was incubated on ice for 30 minutes then subjected to heat shock at 42°C for 30 seconds. Samples were cooled on ice briefly and 950µl of room temperature LB media was added to the transformation reaction. The transformation was incubated at 37°C for 60 minutes under constant agitation. 100 µl of the transformation reaction was then plated onto LB-amp plates.

Individual colonies were picked and streaked onto LB-amp plates and incubated overnight at 37°C. An individual colony from each transformant was then picked and cultured in liquid LB-amp overnight at 37°C under constant agitation. Cultures were then pelleted and plasmid was extracted using plasmid miniprep kit following manufacturer's supplied protocol (Qiagen). Plasmids were then digested with NheI and/or HindIII using previously described methodology and then run on 1% agarose gel as previously described. Positive transformants were then sequenced at University of Pennsylvania DNA Sequencing Facility using their provided instructions.

CsCl Isolation of Plasmid DNA. An individual colony was picked and cultured in 5mL liquid LB-amp media and incubated at 37°C overnight under constant agitation. 5mL culture was used to inoculate 500 ml LB-amp in 2L flask and incubated at 37°C overnight under constant agitation. Culture was centrifuged for 15 minutes at 3000g. Pellet was resuspended in 20mL of resuspension solution (55.5mM glucose, 25mM Tris-Cl, 10mM EDTA, 0.002g/mL lysozyme). Cells were lysed using 40mL of lysis solution (0.16N NaOH and 0.8% SDS) and incubated on ice for 15 minutes. Reaction neutralized using 30mL of neutralizing solution (0.75M potassium acetate and 11.5% glacial acetic acid). Solution was then centrifuged at 4°C for 30 minutes at 5000g. Supernatant was then decanted through four layers of cheesecloth into a new centrifuge bottle. To precipitate out the DNA, 54mL of isopropanol was added and incubated for 10 minutes at room temperature and centrifuged for 30 minutes at 5000g at 4°C. The supernatant was discarded and pellet was washed in 70% ethanol. Pellet was air dried and resuspended in 20mL 1xTE buffer and incubated at 4°C overnight to dissolve the pellet. Solution was then used to dissolve 20g of CsCl and 1.5mL of 10mg/mL ethidium bromide was added. Solution was centrifuged for 15 minutes at 1000g to pellet undissolved ethidium bromide particles. Supernatant was transferred to Beckman Quick-Seal 25x89mm centrifugation tube and overlaid with 20mL of mineral oil. Beckman tubes were heat sealed and centrifuged using Ti70 rotor at 45,000rpm @18C for 48hr.

Beckman tubes were then illuminated with UV light to identify separated bands, the upper plasmid band was extracted using 18 gauge hypodermic needle attached to a

5mL sterile syringe and contents were added to butanol to separate ethidium bromide. Water-butanol phase separation was repeated until clear and liquid layer containing plasmid was then subjected to dialysis in buffer (10mM Tris-HCl pH 8.0, 1mM EDTA) overnight and then purified using phenol-chloroform purification as previously described and concentration was measured by NanoDrop.

PDLSC and GMSC Culturing. Periodontal ligament stem cells, PDLSCs, or Gingival mesenchymal stem cells, GMSCs, passages 1-7 were cultured in MEM-alpha supplemented with 15% fetal bovine serum with 100U/mL penicillin/streptomycin antibiotic solution, 0.1mM L-ascorbic acid phosphate, and 2mM glutamine. Media was replaced every 48 hours during culturing. Cells were incubated at 37°C with a humidified atmosphere of 5% CO2. PDLSCs more than the seventh passage were not used in any of the identified experiments.

Lipofectamine LTX/ STEM/ 2000/ 3000 Transfection. PDLSCs, GMSCs, and 293T cells were plated such that they were 70% confluent at the time of transfection. Lipofectamine reagent based transfection was performed according to manufacturer's provided protocol (ThermoFisher). Cells were plated on 24 well plate and the manufacturer's recommended volume of Lipofectamine reagent plasmid DNA was used per transfection well.

De Novo Infection. Cells to be infected were plated 24 hours prior to infection in either a 6-well or 24-well plate at 1.2×10^6 or 0.24×10^6 cells, respectively. Virion concentration

was calculated through genomic isolation and real-time PCR as previously described. Virus particles were added to each well at a MOI 50 viral copies/cell. Polybrene was added to each to-be infected well at a final concentration of 5mg per milliliter of total media. Cell plates were centrifuged at 450 x g for 1 hour at 25°C and incubated at 37°C with a humidified atmosphere of 5% CO_2 for 2 hours. After the combined total of 3 hours, media was aspirated and replaced with fresh pre-warmed media. Infection rate was monitored and measured visually by use of a Nikon TE2000-U fluorescence microscope to assess GFP expression.

Luciferase Assay. Cells were cultured such that at the time of transfection the cells were 70% confluent by the time of transfection, 24 hours post-transfection the cells were then subjected to KSHV infection. Following 24, 36, and 48 hour timepoints post infection, samples were subjected to luciferase assay with Promega's Dual-luciferase assay kit. Each condition was done in triplicate and each sample was measured in duplicate for both luciferase and renilla levels [25].

Chapter 3

Results:

KSHV affects the expression of several linage specific genes. The Yuan lab has shown that in MSCs, mesenchymal-to endothelial transition (MEndT)-related genes (such as PDPN, EDNRA, PML, PGF and TGF-b3) are up-regulated in response to KSHV infection [15] .

I hypothesize that PROX1 could be upregulated in KSHV infected gingival mesenchymal cells (GMSC), periodontal mesenchymal cells(PDLSC) in comparison to uninfected GMSCs and PDLSCs. To test this human GMSCs and human PDLSCs will be used as well as 293T cells. The human PDLSCs and GMSCs were obtained from patients aged (12-25) years old. They were a kind gift from the Shi lab. Cells from the second and sixth passages were used. They were transfected at 70% confluency using Lipofectamine with PROX1 promoter cloned into a pGL3 promoter. The cells were then infected using recombinant green fluorescent protein (GFP) expressing KSHV (rKSHV.219) The infectivity rate was evaluated by the rate of the cells converted to GFP positive. They were then lysed to be collected at different time points (24,36,48) hours. A luciferase assay was then conducted to measure expression of pPROX1.

Virus purification:

To obtain the KSHV virus iSLK-BAC cells containing KSHV BAC16, derived from the rKSHV.219 virus were cultured. These cells stem from KSHV and Epstein-Barr virus-

coinfected JSC1 primary effusion lymphoma (PEL) cells. KSHV BAC16 virus stock was produced as mentioned in the Materials and Methods section. Six T75 surface 75 cm^2 flasks were used to seed iSLK cells harboring BAC16 at ~70% confluence. They were then treated with 1mM sodium butyrate and 1 µg/ml of doxycycline for 96 hours. The virus-containing supernatants were then collected and concentrated via centrifugation using a SW32 rotor. The residual medium was then used to resuspend the virus pellets. T293 cells were then infected with BAC16 virus stock and analyzed by fluorescence microscopy and flow cytometry at 24 hour post infection.

Viral Titer:

To develop a standard curve from a known control a linearized plasmid containing the KSHV gene Latency Associated Nuclear Antigen, LANA, (3486bp) was used with primers specific to the LANA coding sequence amplifying a 1080bp long region with a known concentration (5ng/ µl). In order to develop a standard curve, the initial sample 1:20 was diluted, such that the first measurement contains 0.25ng of total DNA and proceed in a 1:5 serial dilution for twelve data points, done in triplicate. (Therefore the last data point will only have 5.12E-09 ng total DNA. The results are then plotted such that the Y-axis plots the mean Ct value of the triplicate. Where Ct (cycle threshold) is defined as the number of cycles required for the fluorescent signal to cross the threshold (i.e. exceeds background level). However, the X-axis is not the total DNA concentration of the well, but the $\log_{10}$ value of the total concentration (0.25ng is equivalent to -0.60206).

From here a line was plotted and the formula was calculated for a line (y=mx+b). In this case the slope (m) is -3.3251003 and the y-intercept (b) is 4.73174082. The efficiency of the reaction was calculated through the efficiency formula [10(-1/m)-1]*100, which in this case is 99.8677889%. We can also determine the copy number (number of molecules) for a given concentration of control sample through the formula Molecules=[Xng*6.0221E23]/[(1080bp*617.96g/mol)*10E9ng/g]. Which is simply mass multiplied by Avogadro's number divided by the molecular mass of the DNA sample. While the average molecular mass of one base pair is 660 g/mol for the approximate mass of a whole double-stranded DNA molecule, the exact molecular mass of this LANA sequence is 617.96g/mol as determined by its genetic sequence.

Since we have the known concentration per each data point and the Ct value, we can correlate the copy number (number of molecules) for each Ct value of the standard. With this, the copy number of the unknown KSHV sample at each Ct value in the serial dilution can be determined by reapplying these formulas. Furthermore, the Ct value was plotted against the $\log_{10}$ value of the observed concentration of each sample virus. It was noticed that 1µl of the July virus is 9.46E+05 viroid per microliter. While the August and February samples are 2.21E+06 and 2.51E+06 viroids per microliter, respectively. MOI is related to KSHV by the following formula: Multiplicity of infection (MOI) = KSHV units of virus used for infection / number of cells. Note, for a MOI of 50 for the Yuan's lab's protocol, we require 2.5E+06 viroids per microliter. Which explains why the July KSHV is unable to successfully infect our cell cultures. Given that a 12 well plate has $0.5x10^6$ cells at confluency and is infected by a MOI of 50: $25x10^6$ total KSHV particles

are required. If 10 μl volume of viral solution is used, that must mean the KSHV concentration must be $2.5x10^6$ /ul.

Figure1: Serial dilution of newly purified virus fits to standard curve

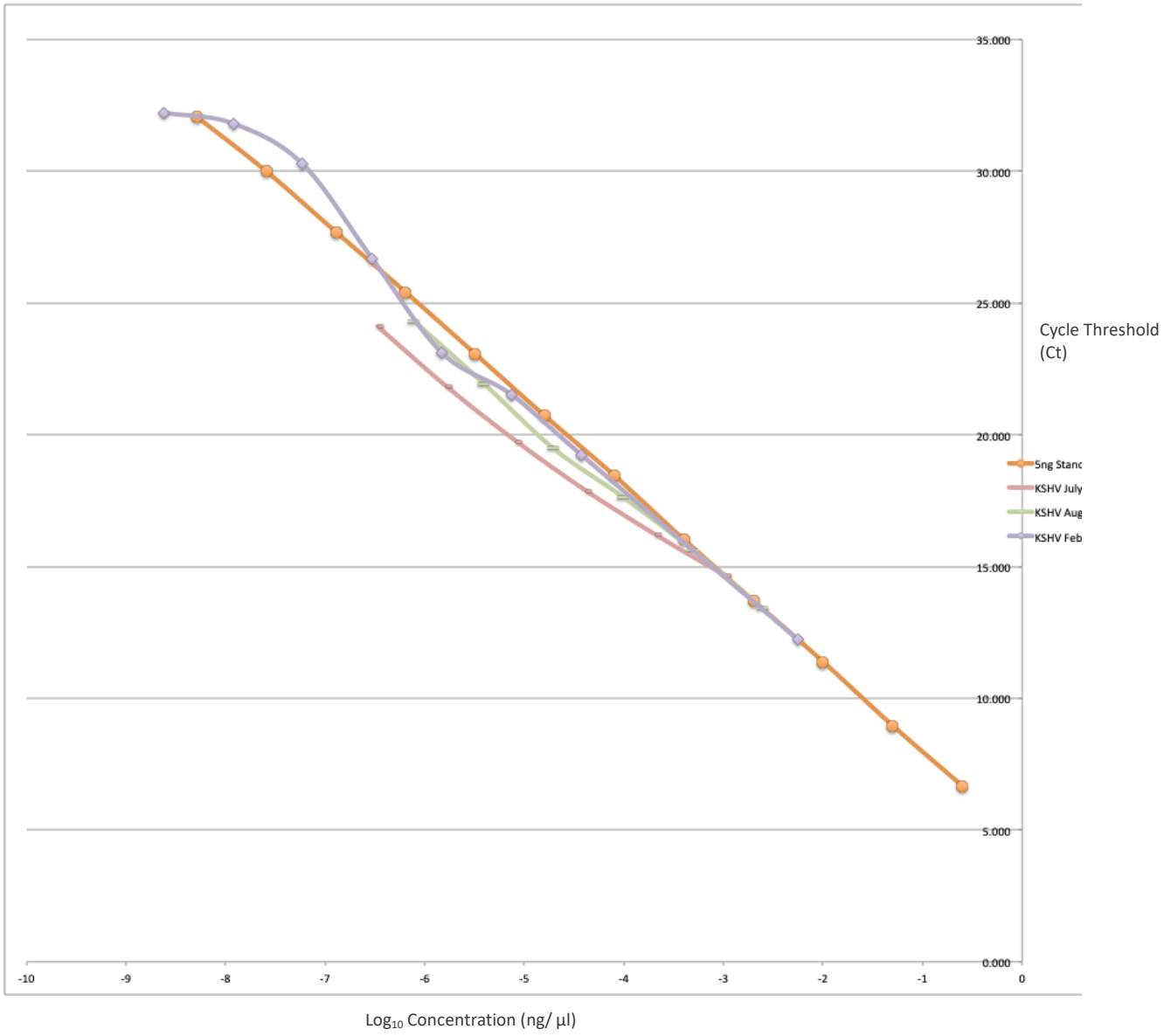

Figure 1: Comparing a 1:5 serial dilution of our lab's LANA standard to three viral DNA samples, also done in a 1:5 serial dilution. The KSHV purification performed in July 2018 was found to be unsuccessful in infecting our cell samples, while both the August and February samples were able to successfully infect our cell samples following a standardized protocol.

Overall infection efficiency:

An infection was done to compare a freshly purified virus (February virus) to a virus previously proven to be effective in the Yuan lab (August virus). The infection efficiency was measured as >90% Infectivity rate was measured by counting the total amount of cells observed in a given visual filed and comparing it to the amount of GFP positive cells observed within the same visual field if n=100 cells and 80 cells were GFP positive then 80/100 =80%. The cells were evaluated at different time points. **Figure 2 and Figure 3** An experiment was conducted to evaluate the infection efficiency in PDLSCS,GMSCS, and 293 cells**. Figure 4**

Figure 2: Comparing August virus to February virus infectivity rate in PDLSCs

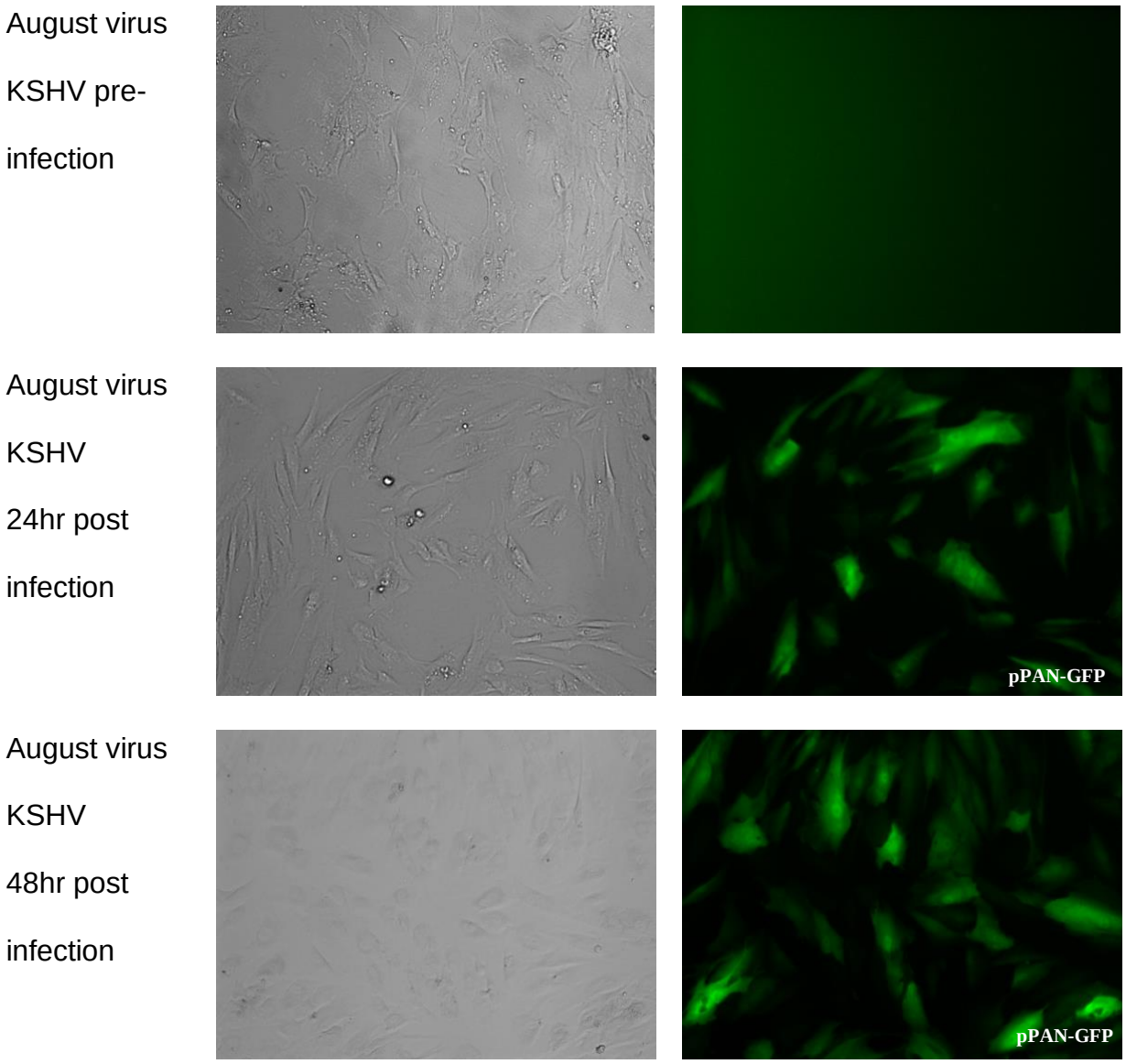

Figure 2: August virus is able to successfully infect PDLSCs. Cells are imaged using a 10x/0.25 objective inverted fluorescent light microscope.

Figure 3: Comparing August virus to February virus infectivity rate in PDLSCs

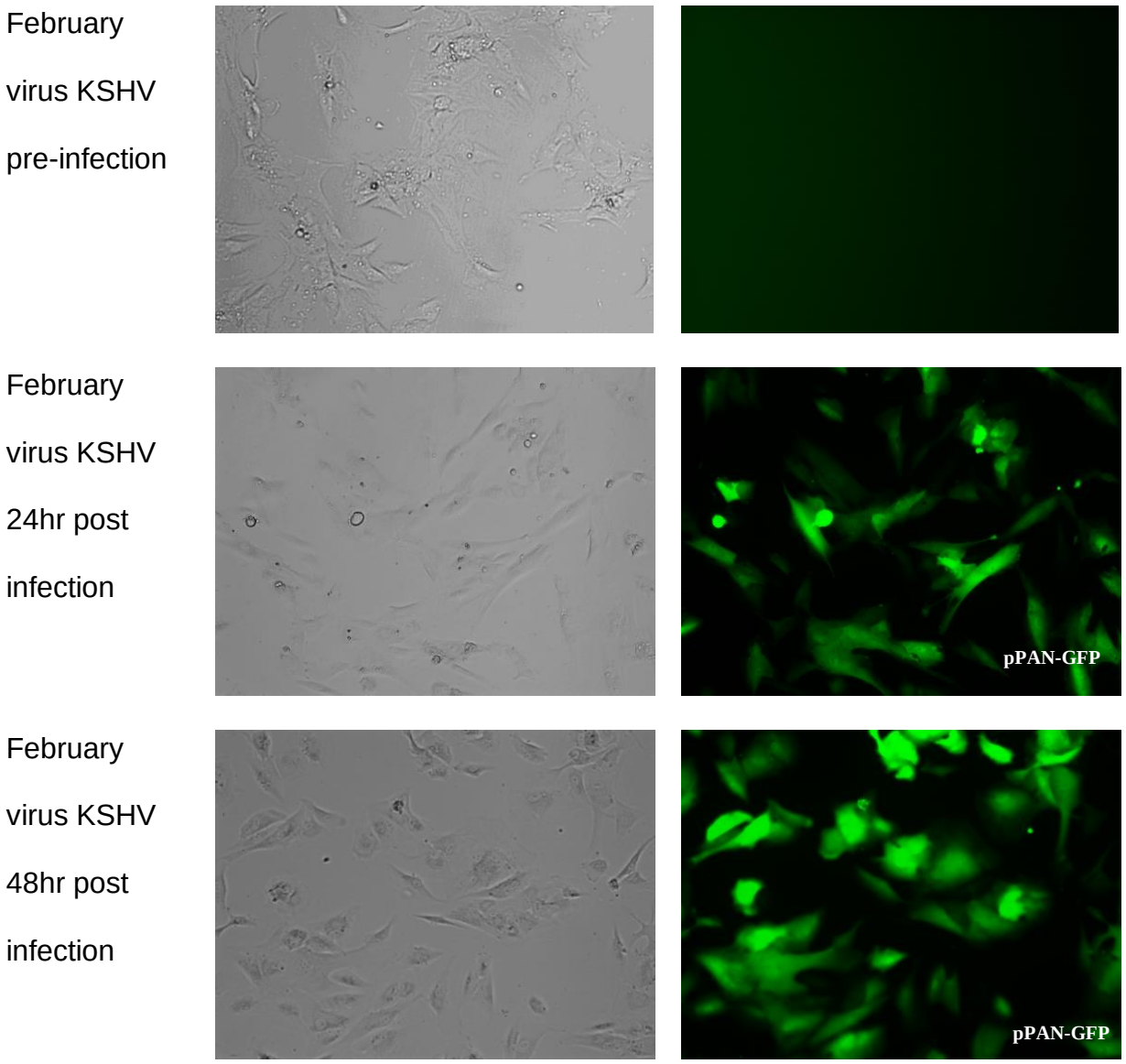

Figure3: February virus is sucessfully able to infect PDLSCs. Cells are imaged using a 10x/0.25 objective inverted fluorescent light microscope.

Figure 4: February virus is able to establish a successful infection in PDLSCs, GMSCs, and 293T cells

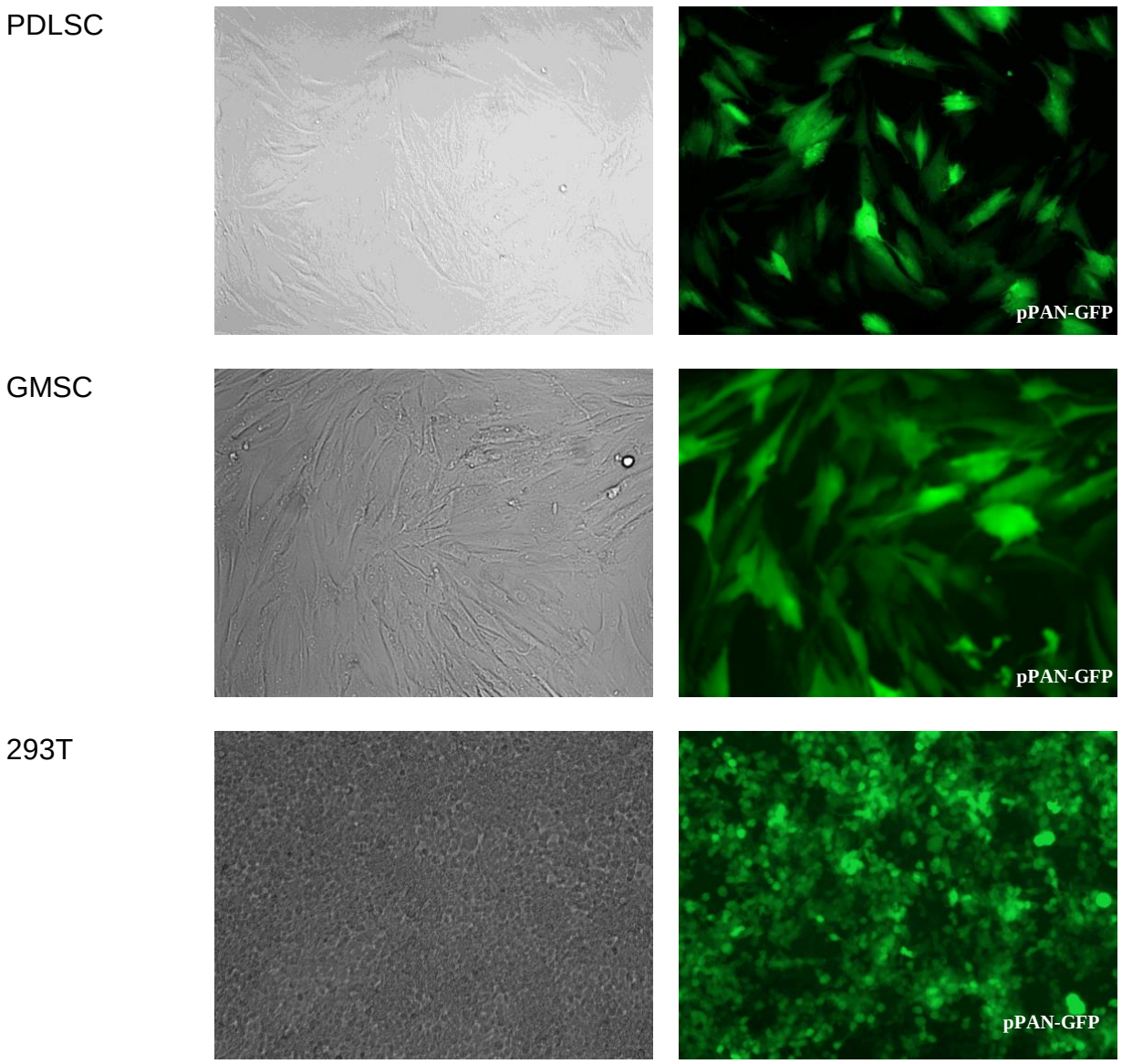

Figure 4: The February virus infection efficiency in PDLSC:80%, GMSC:90%, and 293T cells 90%.n=100 cells. Cells are imaged using a 10x/0.25 objective inverted fluorescent light microscope.

Cloning:

The promoter region of PROX1 (pPROX1) was cloned into a luciferase reporter plasmid via sticky end ligation. pGL3 was chosen due to the luciferase coding sequence in the pGL3 vector which contains an upstream multiple cloning site, MCS. By cloning pPROX1 into the MCS of pGL3 we were able to determine whether pPROX1 has been activated in a selected cell line. The pPROX1 area was identified through the Ensemble database and through a study conducted by Zhaou et al.[26] Seven versions of pPROX1 were used before finding the correct promoter region. The ones that were used throughout the experiment were version 6 and version 7. They were confirmed using sequencing. The primers were designed making sure the Forward primer contains a 5' Nhe1 digest site with a CCCC upstream sequence to aid in restriction enzyme digest. Alternately, the Reverse primer was designed to contain a downstream HindIII digest site with a 5' CCCC sequence. By selecting Nhe1 and HindIII for a 'sticky end' ligation approach directionality of the insert upon ligation with the pGL3 vector was ensured. Some of the complications faced when conducting the experiment were locating a pGL3 WT vector, a previously modified vector had to be used. The available pGL3 vector contained a foreign piece of DNA. Through sequencing it was confirmed that the area of the foreign DNA was the only modified area. The foreign insert was flanked by a NheI and two HindIII digest sites, therefore a double Nhe1 and HindIII digest had to be done followed by a phosphatase (CIP) reaction. Through performing a CIP reaction, re-ligation of the unwanted pre-existing promoter region was prevented. Also, rather than a gel extraction for the vector, phenol-chloroform DNA precipitation was only done to maintain a high yield and prevent degradation to the vector. Another issue that was

faced was that the pPROX1 region contains numerous long C and G repeats which made PCR amplification very difficult for the upstream region. Therefore a shortened ~2kb region that is directly upstream of the ATG codon was used.

Due to early issues with the purity of the PCR product by using Promega GoGreen Taq polymerase and unsuccessful T4 Ligations, even after phenol-chloroform precipitation of the samples, we chose to first clone in the promoter regions into pCR2.1 using TA ligation where the vector is from a commercially pre-prepared; pCR2.1 comes linearized with T-overhangs.

V6 and V7 were successfully TA cloned into pCR2.1. Furthermore, a successful ligation and transformation by screening transformant colonies using NheI and/or HindIII digest was confirmed. Note, pCR2.1 has a pre-existing HindIII digest site in the multiple clone site region, MCS, so HindIII digest alone will show a double band pattern when running the sample on an agarose gel electrophoresis if the promoter(s) are cloned into the proper forward running orientation, **Figure 5a**. From there we were able to transform our novel pCR2.1-pPROX1 v6 & v7 plasmids into competent cells and perform a plasmid preparation for NheI & HindIII restriction enzyme digest and agarose gel band extraction to continue with our ligation strategy. Once the purified digested promoters were obtained, sticky-end ligation using T4 DNA Ligase and the NheI+HindIII digested pGL3 vector was done, which was followed by transforming the ligation reactions into competent cells. Similar to the pCR2.1-pPROX1 v6 & v7 screening methodology, the potential transformant colonies were screened through NheI+HindIII restriction enzyme

digest of prepared plasmid samples and gel electrophoresis, and validated by sequencing the plasmid samples through the Penn Genomics Analysis Core. **Figure 5**

Figure 5 Successful cloning of pPROX1 V6/V7 into pCR2.1 and pGL3

a.

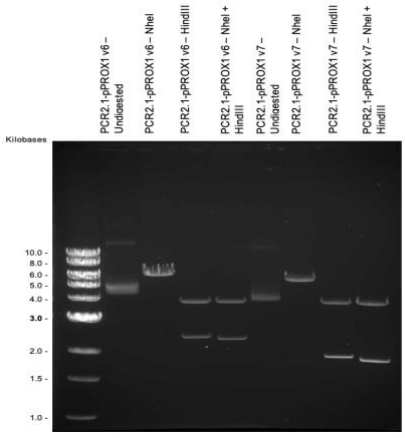

b.

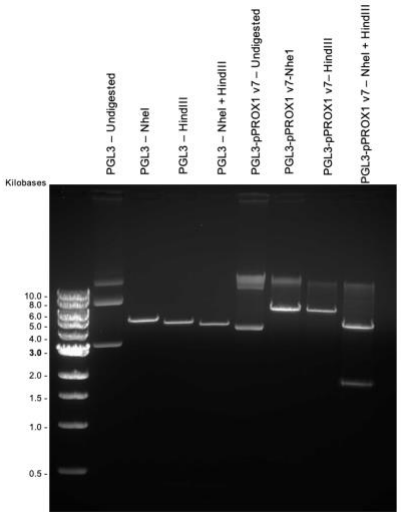

c.

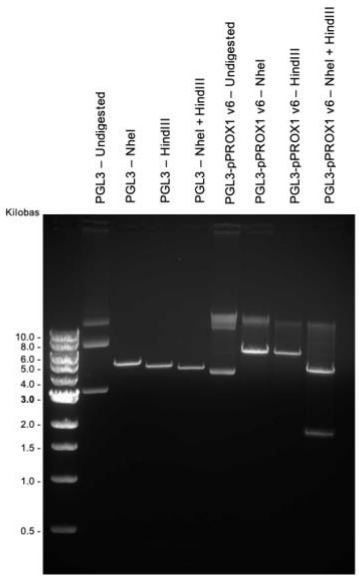

Figure 5 a. The pCR2.1vector is 4029bp or 4.0kb **b.** v7 is 1801 or 1.8kb, note that the forward primer's consensus sequence starts 97bp upstream of V6 forward primer's consensus sequence. pGL3 vector is 4818bp or 4.8kb **c.** V6 is 2320bp or 2.3kb

Transfection:

After cloning the pGL3-pProx1 v6 and v7 vectors. The next step was to co-transfect the pRL vector which is wild-type Renilla luciferase (Rluc) control reporter vector, along with the newly constructed pGL3 vectors into 293T cells, PDLSCs, and GMSCs. However, similar to other stem cells, MSCs are challenging to transfect, and therefore standardizing a simple transfection protocol for MSCs is essential.[27] In order to standardize a simple protocol for transfection of MSCs, we conducted a series of experiments to establish a protocol that does not require the use of specific expensive equipment or viral particles. A variety of lipofectamine products were used and a reporter pMAX-GFP was used to test their efficiency in 293T, PDLSCs, and GMSCs. Lipofectamine contains lipid subunits that can form liposomes where each product consists of different formulations of cationic liposomes and neutral co-lipids that have varying efficiencies across different cell lines. Transfections were done using Lipofectamine 2000, 3000, LTX, and STEM. The transfection was done in accordance to the provided manufacture's protocol. They were done using various amounts of lipofectamine in triplicate to assess the proper volume of lipofectamine necessary for the highest transfection efficiency possible and the least cytotoxic effects. Transfection efficiency was measured by counting the total amount of cells observed in a given visual filed and comparing it to the amount of GFP positive cells observed within the same visual field, for example if n=100 cells overall were counted and 80 cells were GFP positive then 80/100 =80%.

Comparing lipofectamine transfection reagents:

Measuring transfection efficiency using Lipofectamine Stem (LipoStem) Figure 6,7, Lipofectamine 2000 Figure 8, Lipofectamine LTX with PLUS Reagent Figure 9,10,11 and Lipofectamine 3000 Figure12,13 in PDLSCs using pMAX-GFP and different volumes of the lipofectamine reagent as per the manufactures protocol.

Figure 6: Lipofectamine Stem shows high cell toxicity and low transfection efficiency at 1µL of lipofectamine reagent per well in a 24 well plate

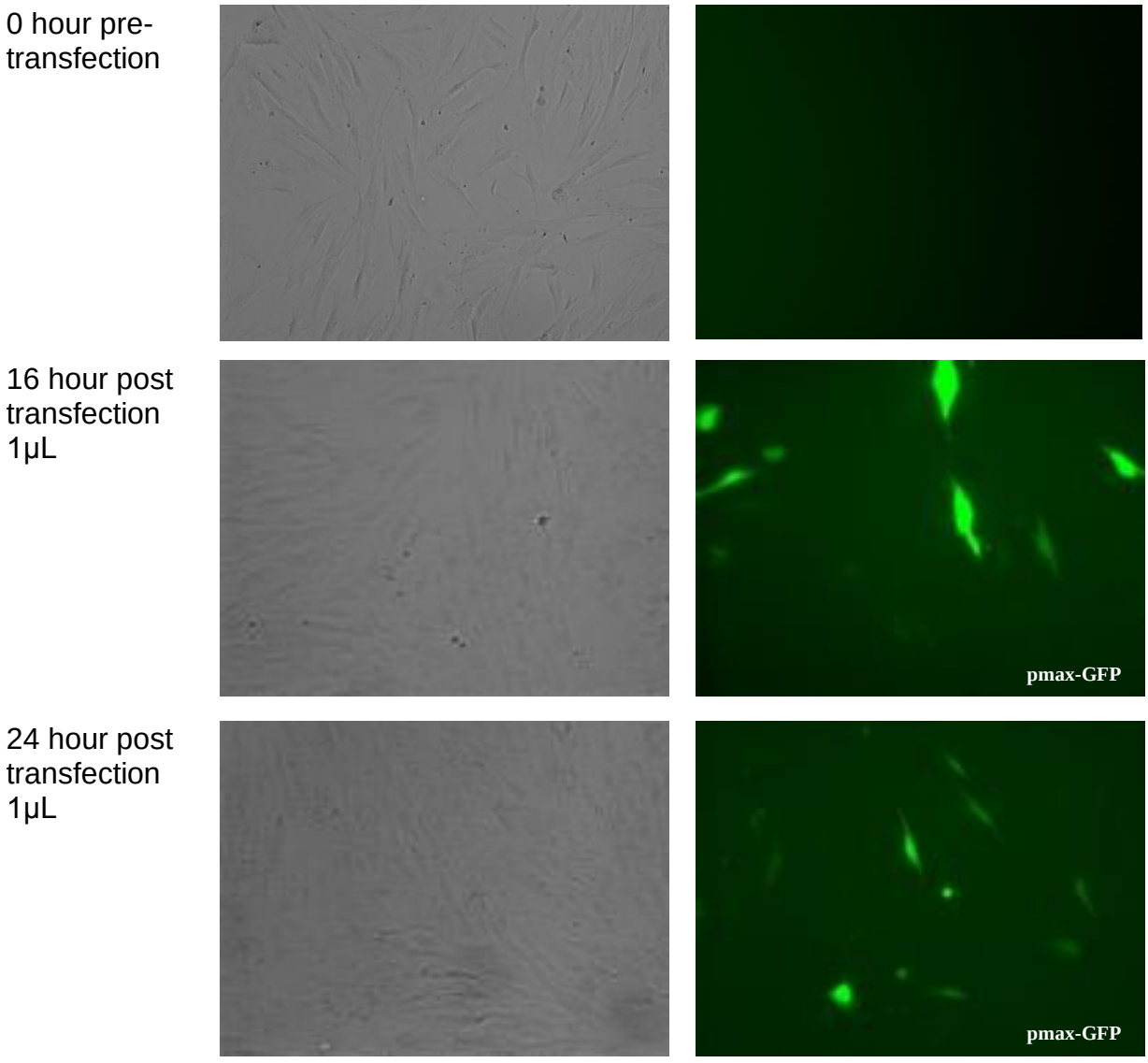

Figure 6: Lipofectamine STEM results in high cell toxicity and low transfection efficiency: 40% n=100 cells. Cells are imaged using a 10x/0.25 objective inverted fluorescent light microscope.

Figure 7: Lipofectamine Stem shows high cell toxicity and low transfection efficiency at 1µL of lipofectamine reagent per well in a 24 well plate.

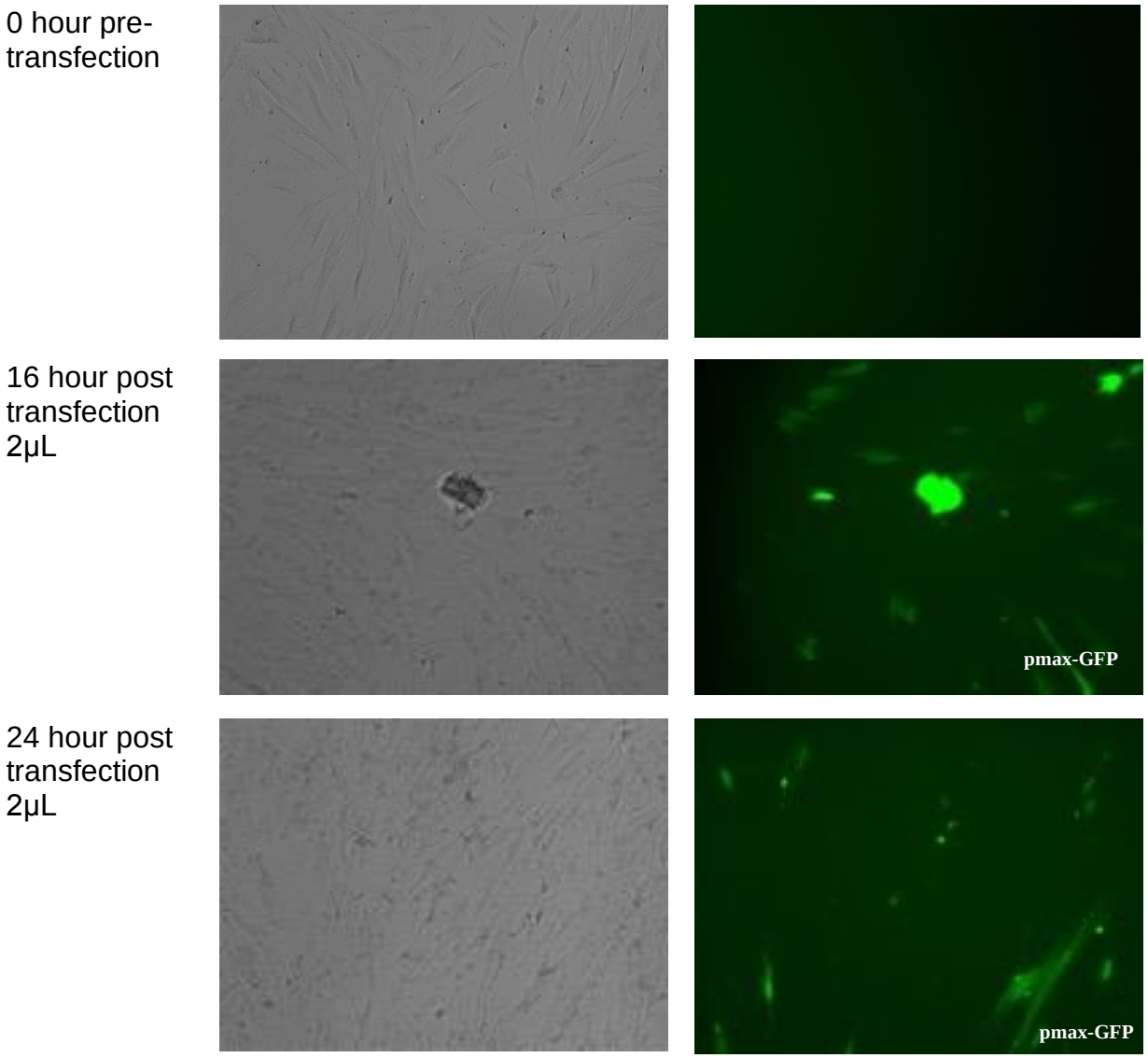

Figure 7: Lipofectamine STEM results in high cell toxicity and low transfection efficiency: 40% n=100 cells. Cells are imaged using a 10x/0.25 objective inverted fluorescent light microscope.

Figure 8: Lipofectamine 2000 shows high cell toxicity and low transfection efficiency at 2µL of lipofectamine reagent per well in a 24 well plate.

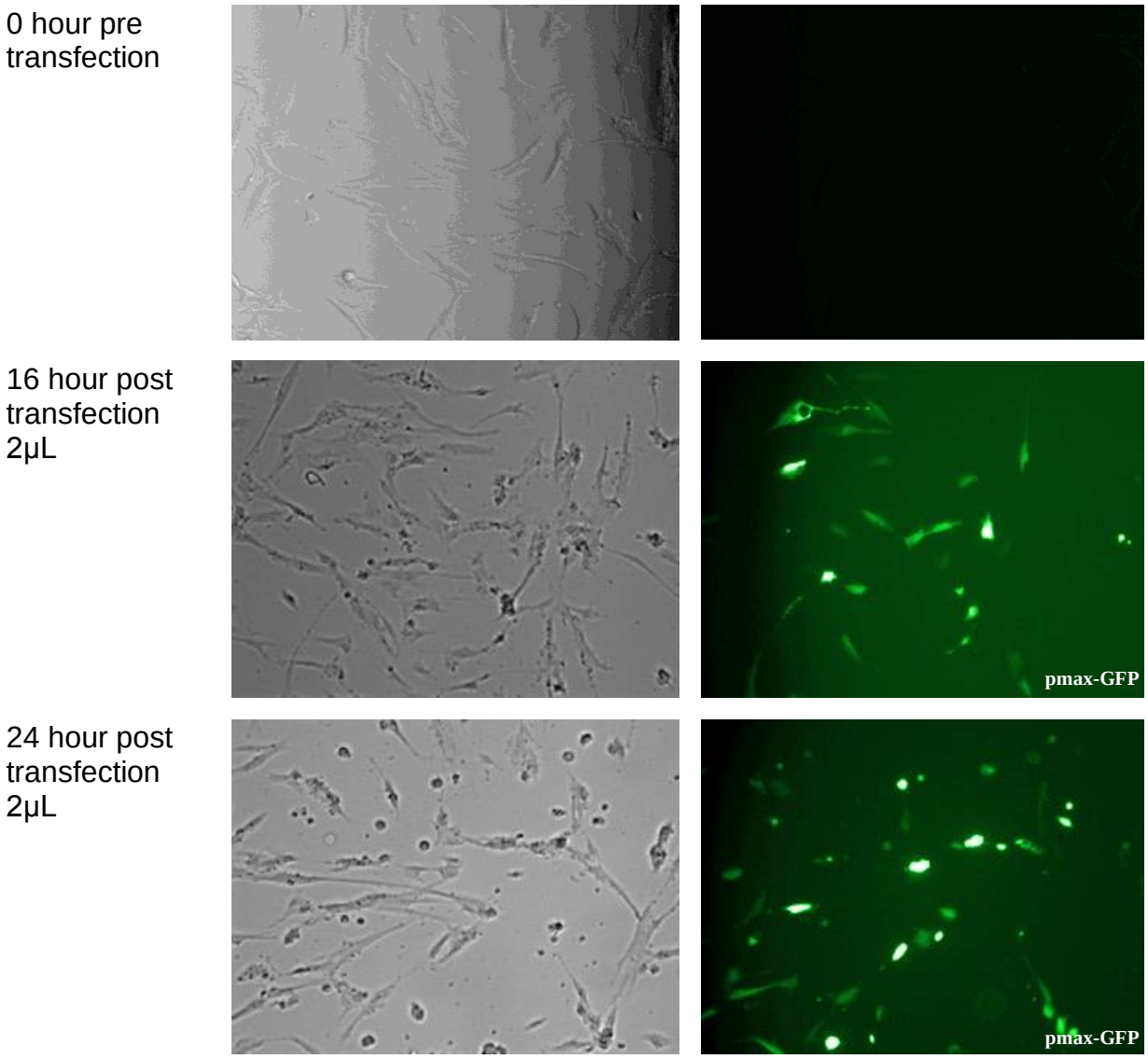

Figure 8: Lipofectamine 2000 results in high cell toxicity and low transfection efficiency: 10% n=100 cells. Cells are imaged using a 10x/0.25 objective inverted fluorescent light microscope.

Figure 9: Lipofectamine LTX with PLUS shows high cell toxicity and low transfection efficiency at 1µL of lipofectamine reagent per well in a 24 well plate.

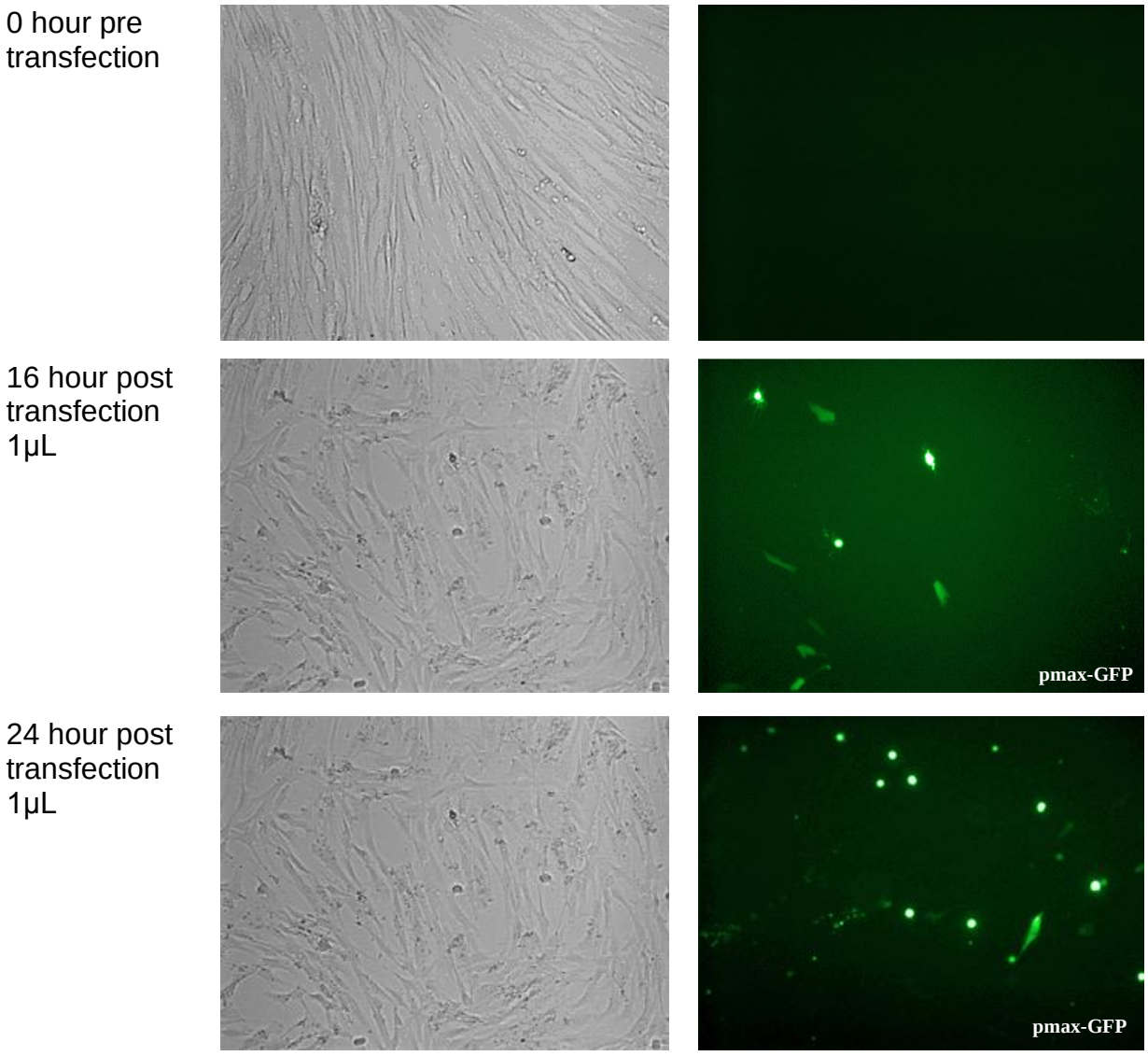

Figure 9: Lipofectamine LTX results in high cell toxicity and low transfection efficiency: 10% n=100 cells. Cells are imaged using a 10x/0.25 objective inverted fluorescent light microscope.

Figure 10: Lipofectamine LTX with PLUS shows high cell toxicity and low transfection efficiency at 1.5µL of lipofectamine reagent per well in a 24 well plate

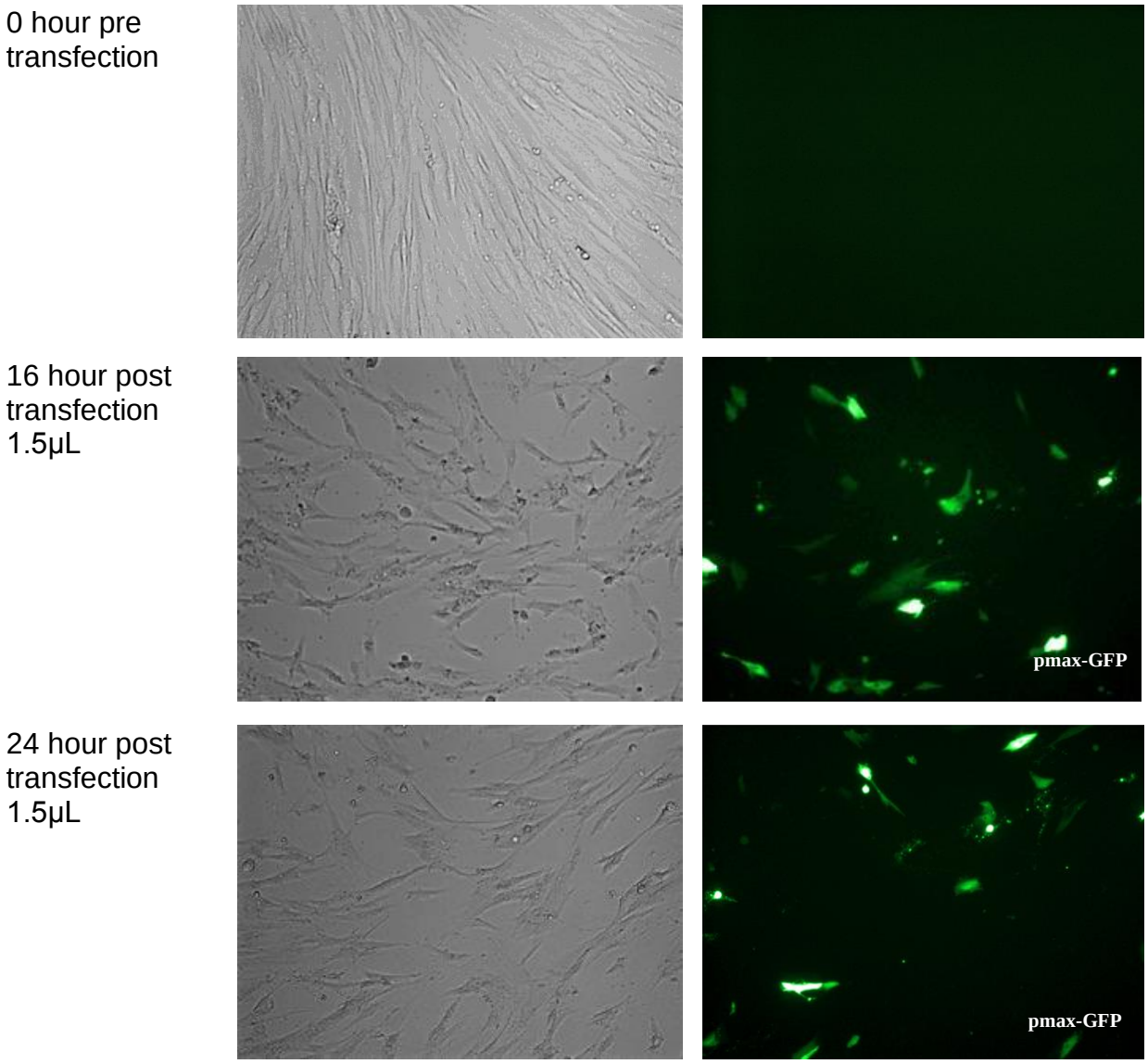

Figure 10: Lipofectamine LTX results in high cell toxicity and low transfection efficiency: 10% n=100 cells. Cells are imaged using a 10x/0.25 objective inverted fluorescent light microscope.

Figure 11: Lipofectamine LTX with PLUS shows high cell toxicity and low transfection efficiency at 2µL of lipofectamine reagent per well in a 24 well plate

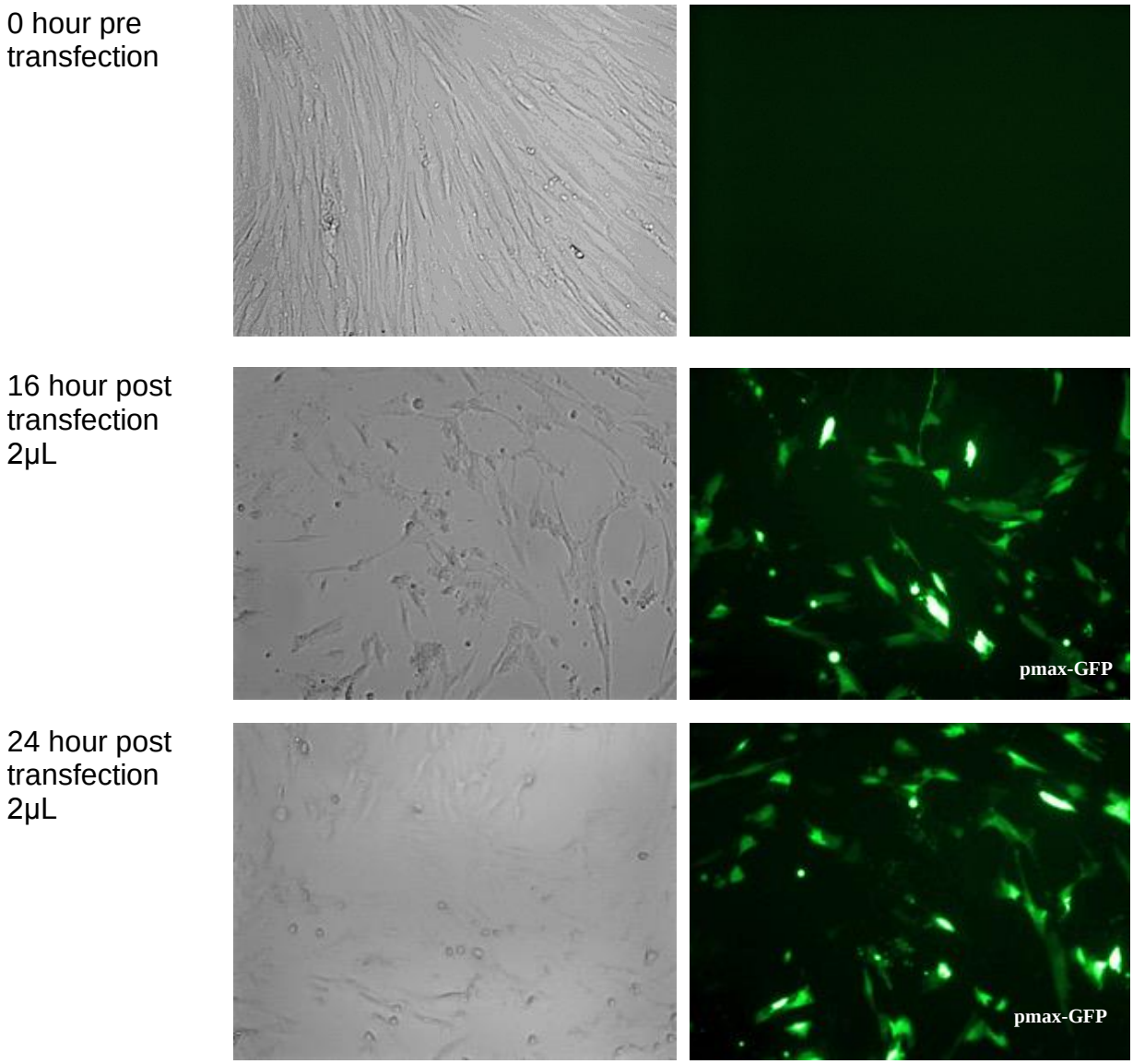

Figure 11 : Lipofectamine LTX results in high cell toxicity and low transfection efficiency: 10% n=100. Cells are imaged using a 10x/0.25 objective inverted fluorescent light microscope.

Figure 12: Lipofectamine 3000 shows the best results in comparison to other lipofectamine reagents 0.75µL of lipofectamine reagent per well in a 24 well plate.

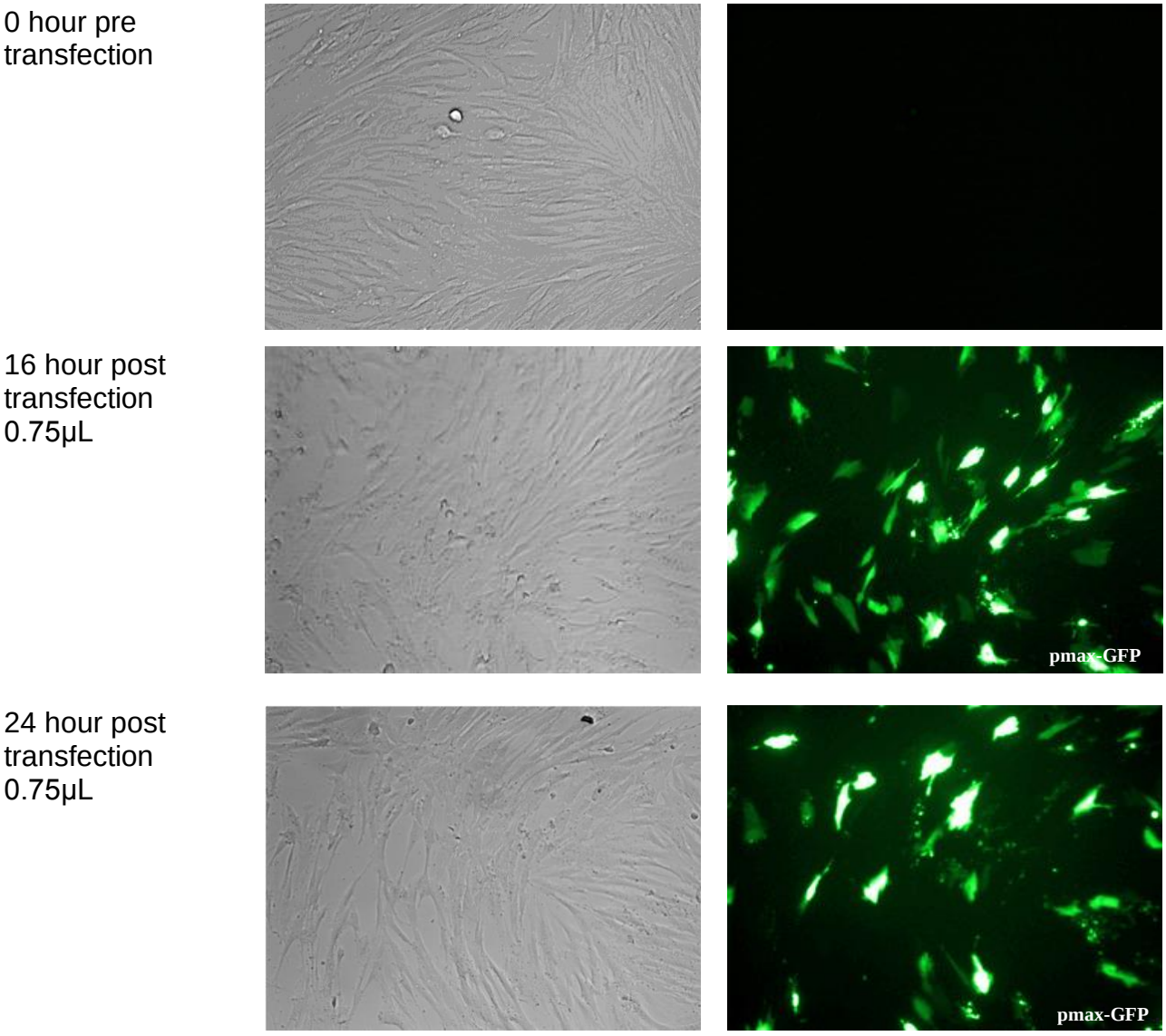

Figure 12: Lipofectamine 3000 shows low cell toxicity and high transfection efficiency 70% n=100 cells. Cells are imaged using a 10x/0.25 objective inverted fluorescent light microscope.

Figure 13: Lipofectamine 3000 shows the best results in comparison to other lipofectamine reagents when using 0.75µL of lipofectamine reagent per well in a 24 well plate. 1.5µL shows a decreased transfection efficiency and higher cell toxicity in comparison to 0.75µL of lipofectamine reagent per well in a 24 well plate.

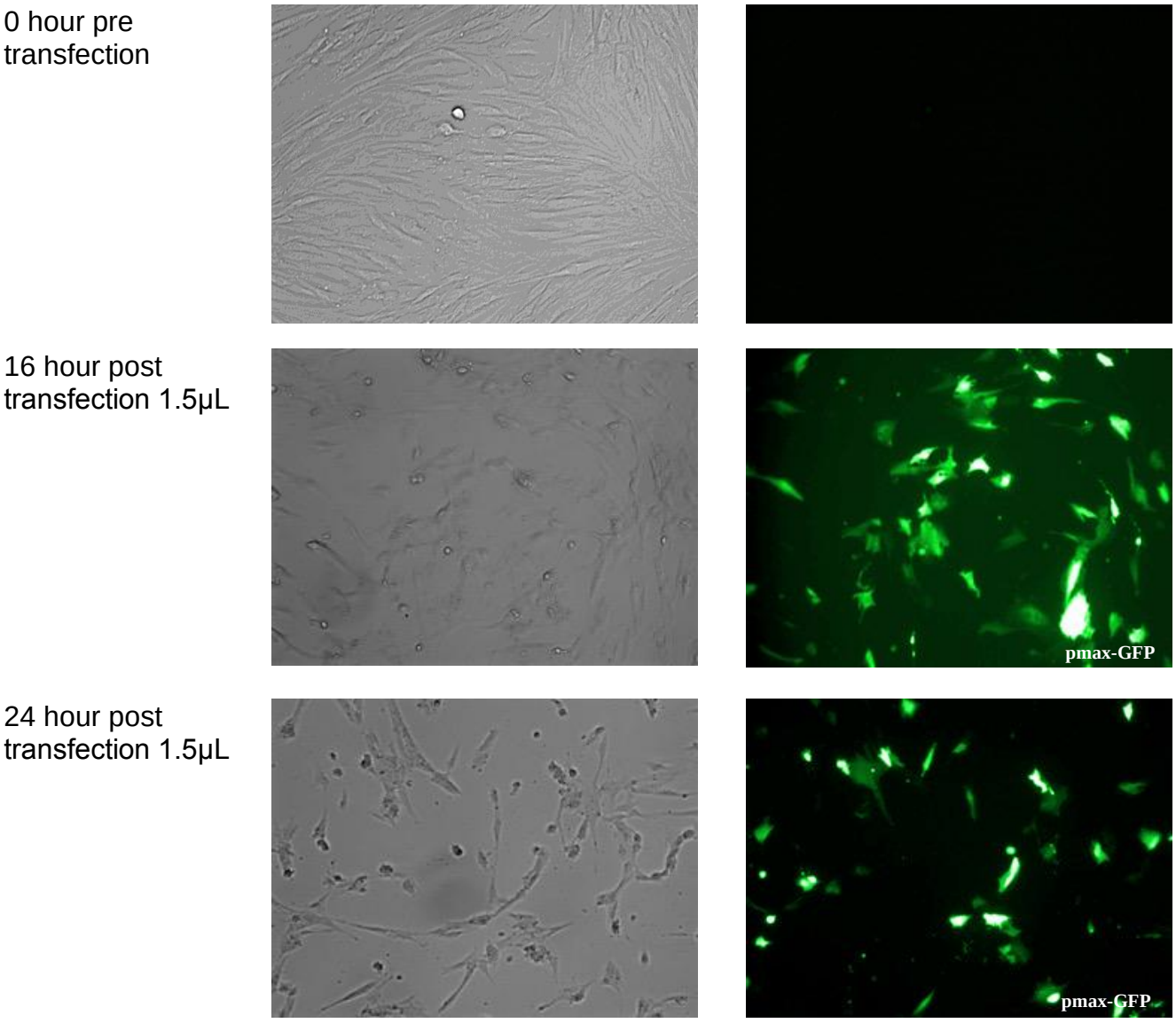

Figure 13: Lipofectamine 3000 results in low cell toxicity and high transfection efficiency: 60% n =100 cells. Cells are imaged using a 10x/0.25 objective inverted fluorescent light microscope.

Lipofectamine 3000 Transfection Reagent has been proven to be have the least amount of cell toxicity and the highest transfection efficiency in PDLSCs. To confirm this, a transfection was done using 0.75µL of Lipofectamine 3000 per well of a 24 well plate. This experiment was conducted to compare transfection efficiency across PDLSC, GMSC, 293T cell lines using pMAX-GFP. **Figure14,15,16,17**

Figure 14: 0.75µL of lipofectamine reagent per well in a 24 well plate. Lipofectamine 3000 - 0 hour pre-transfection

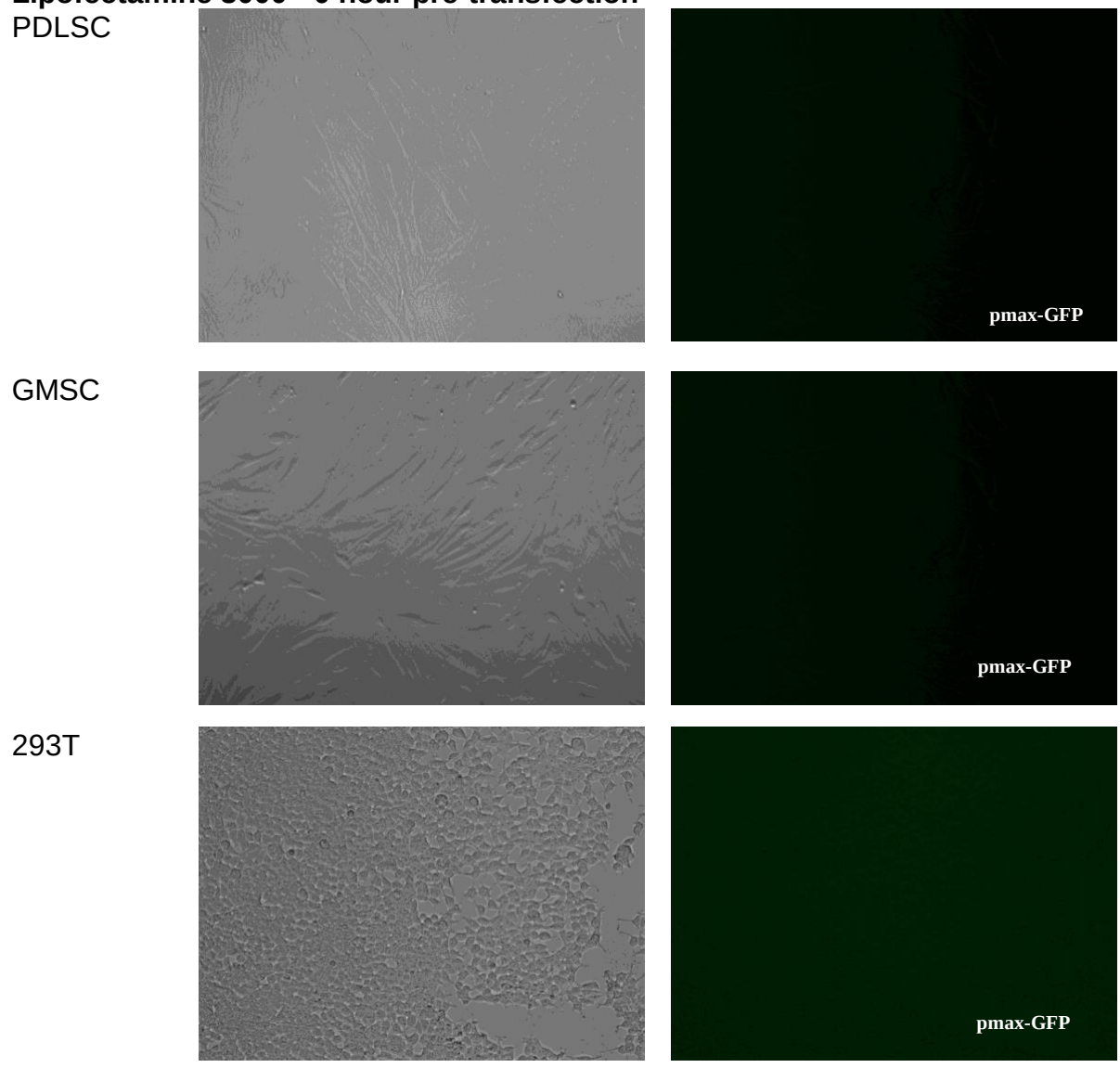

Figure14: Lipofectamine 3000 results in low cell toxicity and high transfection efficiency: 60% n=100 cells. Cells are imaged using a 10x/0.25 objective inverted fluorescent light microscope.

Figure15:Lipofectamine 3000 0.75µL of lipofectamine reagent per well in a 24 well plate – 24 hours post transfection.

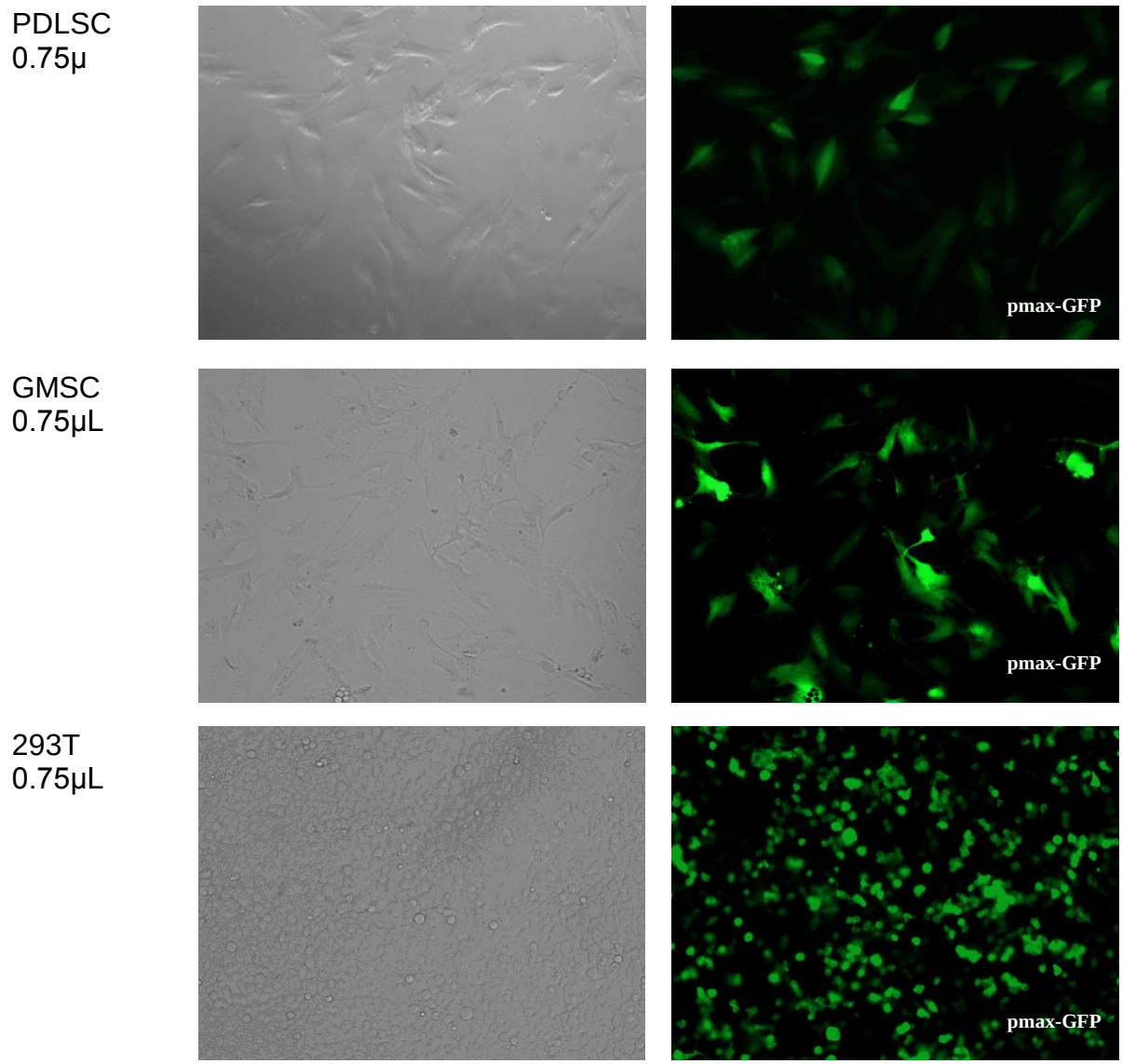

Figure15: Lipofectamine 3000 0.75µL of lipofectamine reagent per well in a 24 well plate results in low cell toxicity and high transfection efficiency in PDLSC 70% GMSC: 80% 293T: 90% n=100 cells. Cells are imaged using a 10x/0.25 objective inverted fluorescent light microscope.

Figure16: Lipofectamine 3000 0.75µL of lipofectamine reagent per well in a 24 well plate – 36 hours post transfection.

PDLSC

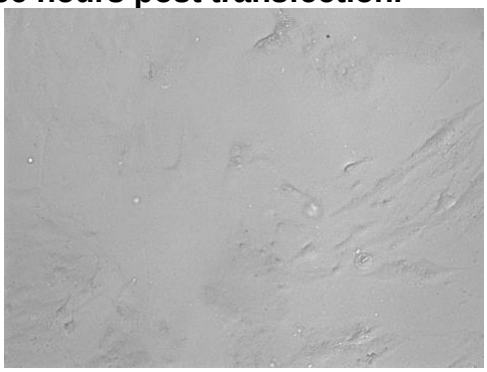

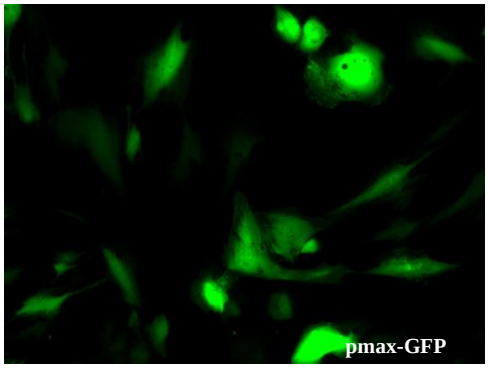

GMSC

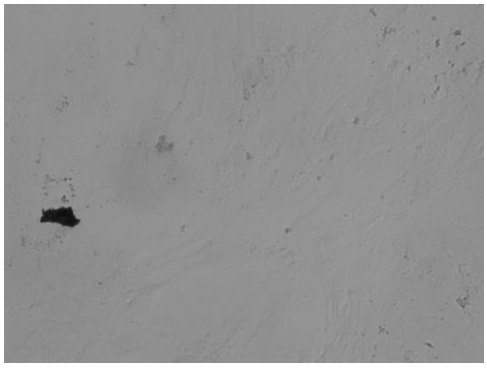

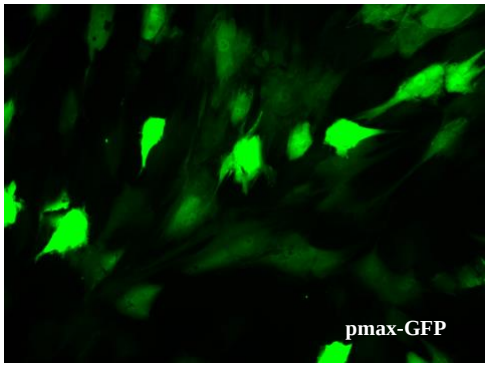

293T

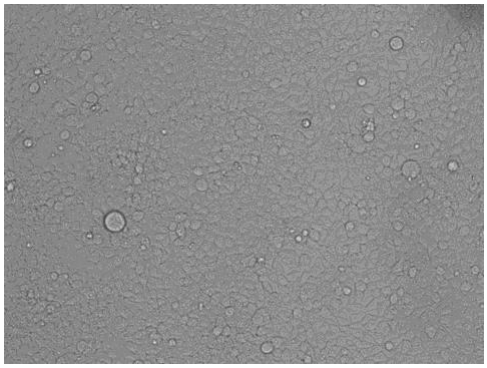

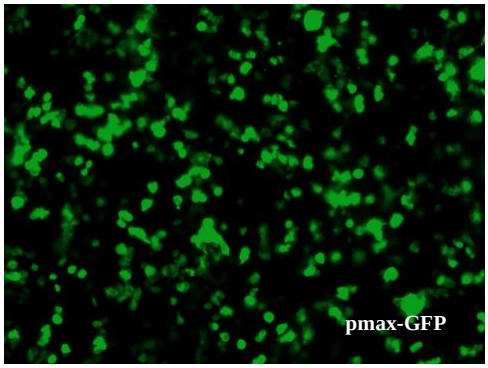

Figure16: Lipofectamine 3000 0.75µL of lipofectamine reagent per well in a 24 well plate results in low cell toxicity and high transfection efficiency in PDLSC 70% GMSC: 80% 293T: 90% n=100 cells. Cells are imaged using a 10x/0.25 objective inverted fluorescent light microscope.

Figure 17: Lipofectamine 3000 0.75µL of lipofectamine reagent per well in a 24 well plate – 48 hours post transfection.

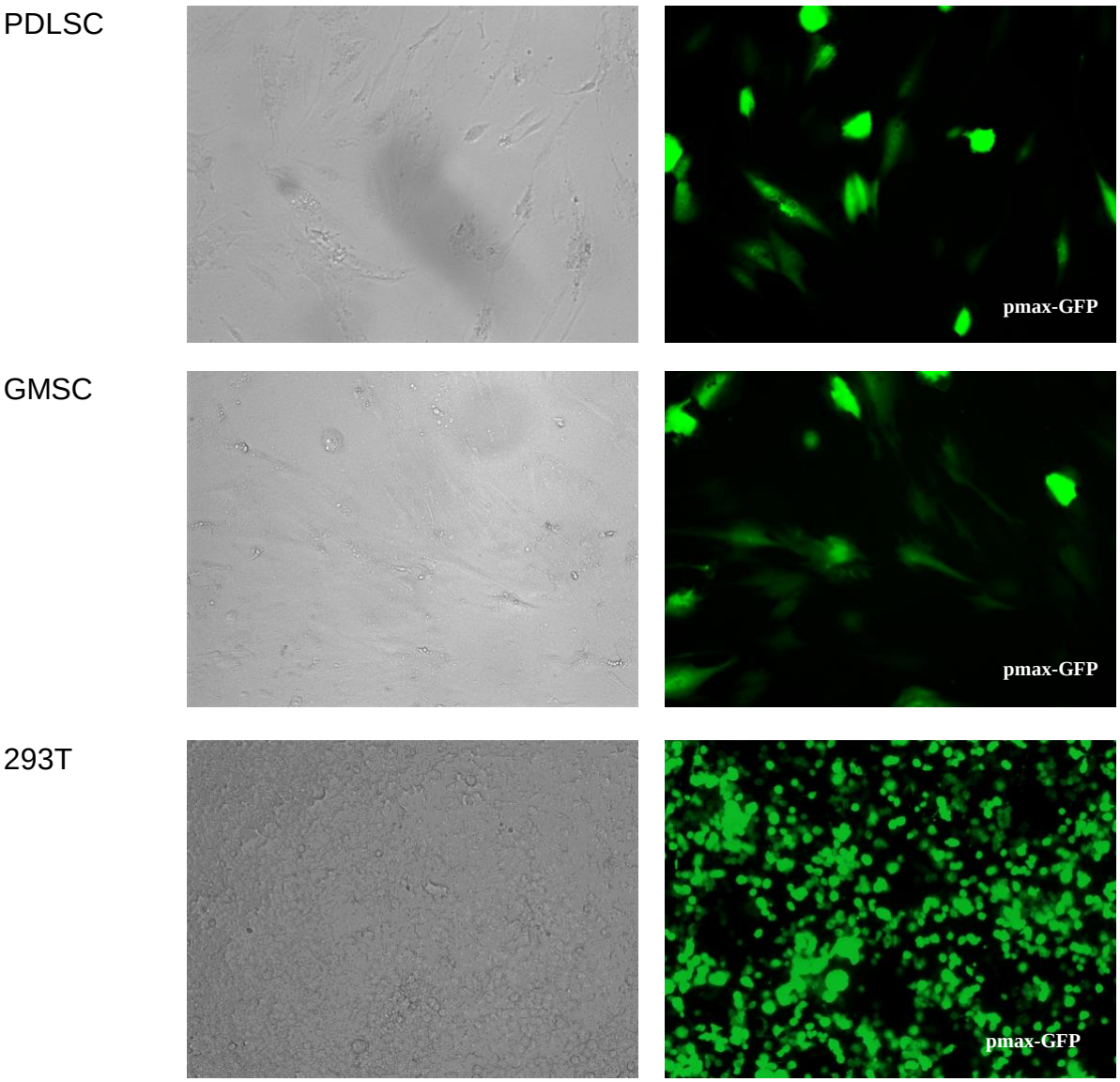

Figure 17 : Lipofectamine 3000 results in low cell toxicity and high transfection efficiency in PDLSC 70% n 100 GMSC: 80% 293T: 90% n=100 cells. Cells are imaged using a 10x/0.25 objective inverted fluorescent light microscope.

Luciferase assay results:

A successful transfection through the use of the pMAX-GFP reporter vector has been confirmed. Also, we were able to confirm a successful co-transfection by having a consistently higher firefly to renilla ratio in the pGL3-pPAN KSHV+ infected 293T samples when compared to its uninfected counterpart, which was expected since the KSHV PAN promoter is transcriptionally active in either the lytic or latent lifecycle of KSHV [28]. Although we were able to achieve a successful transfection, with minimal cytotoxicity, and show that we were able to successfully perform a luciferase assay using pGL3-pPAN, we were unable to detect a luciferase signal above the background noise threshold when using pGL3-pPROX1 version 6 or 7 regardless of KSHV infection.

Figure 18.19.20

Figure18: 293T: KSHV infected cells do not exhibit noticeable luciferase signal activation of pPROX1 at 24, 36, and 48 hours post infection.

a.

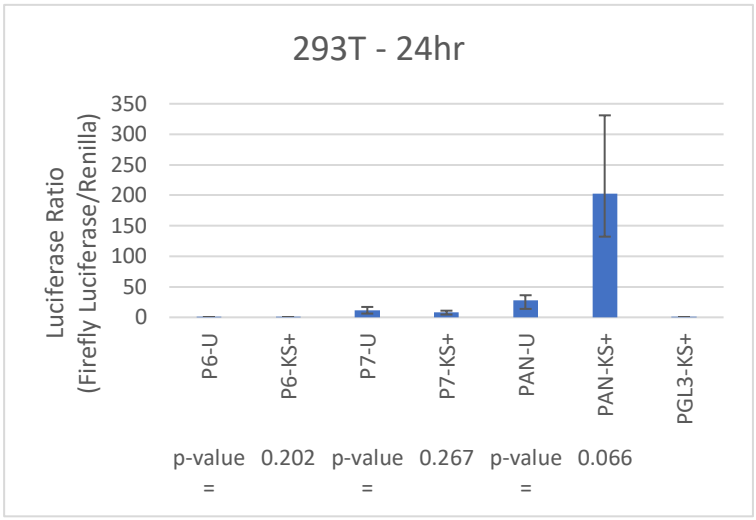

b.

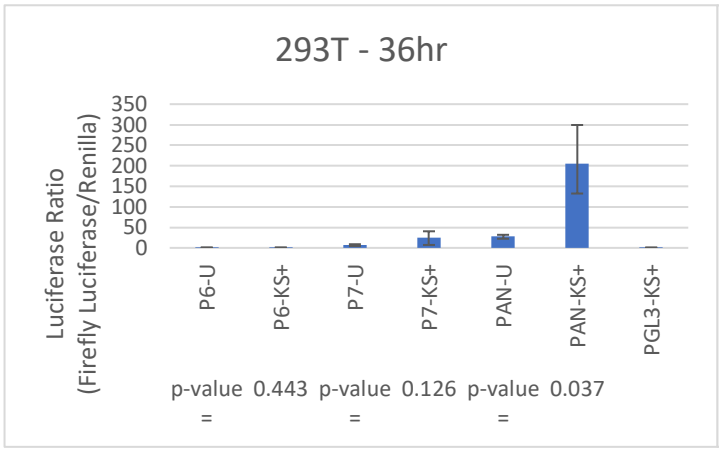

c.

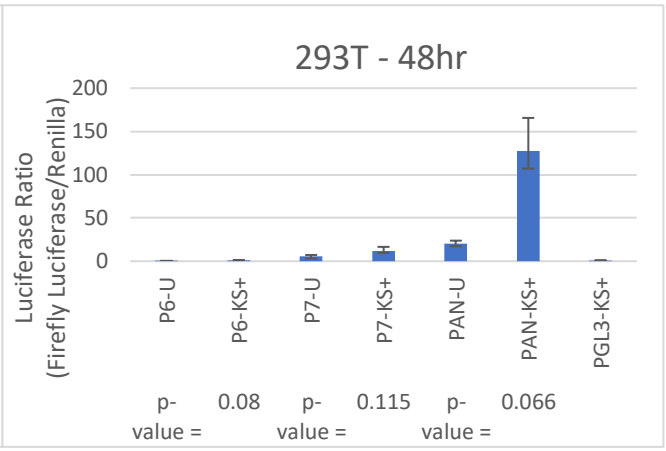

Figure 18: a. Both v6 and v7 of the pPGL3-pPROX1 conditions did not exhibit noticeable luciferase signal. KSHV infected 293T cells transfected with pGL3-pPAN exhibited a positive luciferase signal compared to renilla. Most likely due to a wide variation of signal across samples, the results remained statistically insignificant with a p-value greater than 0.05.
b. KSHV-infected 293T cells transfected with pGL3-pPAN showed an increase in luciferase signal compared to the uninfected control with a p-value less than 0.05 **c.** KSHV infected 293T cells transfected with pGL3-pPAN exhibited a positive luciferase signal compared to renilla. Due to an increase in luciferase signal in the uninfected pGL3-pPAN sample, the results remained statistically insignificant with a p-value greater than 0.05.

Figure19: PDLSCs: A slight increase in luciferase signal in KSHV+ pGL3-PROX1 v6 is observed at 24,36 and 48 hours post infection.

a.

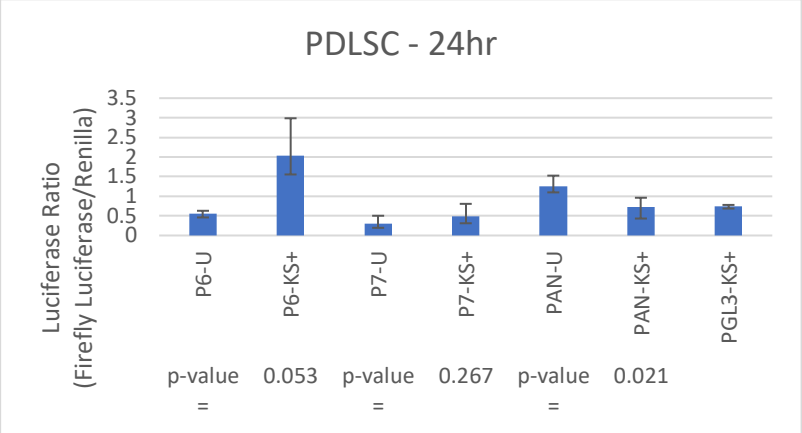

b.

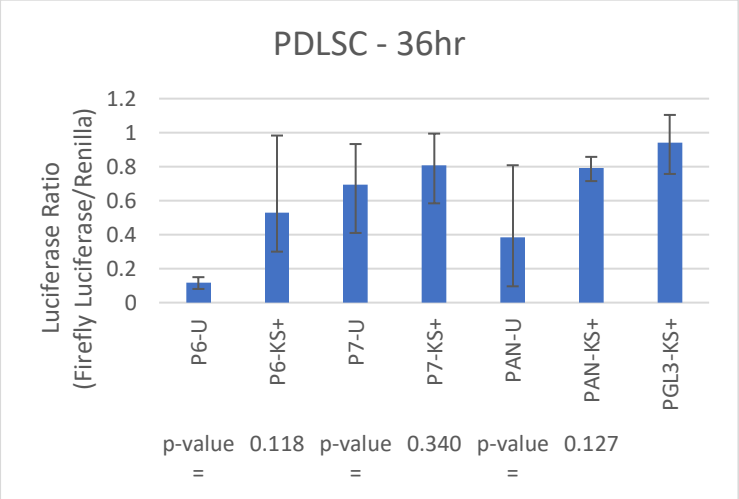

c.

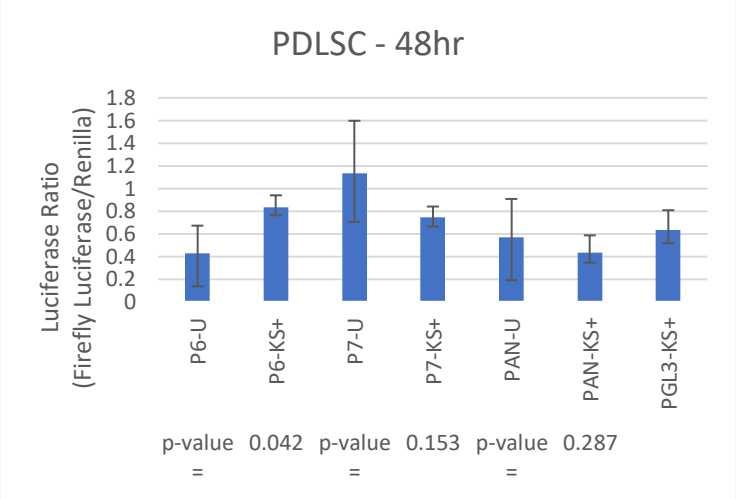

Figure 19: a. We observed an increase in luciferase signal with the PGL3-pPROX1 version 6 construct following KSHV infection, Unexpectedly, the PGL3-pPAN uninfected condition showed a higher luciferase ratio than the infected counterpart. But, both the uninfected and infected PGL3-PAN luciferase to renilla ratio is similar to that of the PGL3 empty vector control, suggesting that this observation is due to background noise. **b.** We see an increase in luciferase signal in KSHV+ pGL3-PROX1 v6. **c.** Again we see an increase in luciferase signal in KSHV+ pGL3-PROX1 v6, unlike the v7 conditions which exhibited a luciferase signal pattern opposite to our expectations. But, v6 uninfected, v7, PAN, and PGL3 empty vector all show almost similar results suggesting background noise interference.

Figure 20: GMSCs: KSHV infected cells do not exhibit noticeable luciferase signal activation of pPROX1 at 24,36 and 48 hours

a

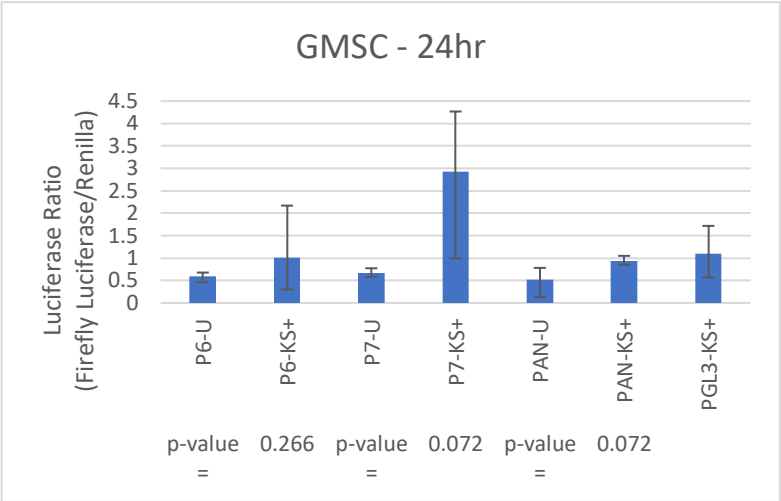

b.

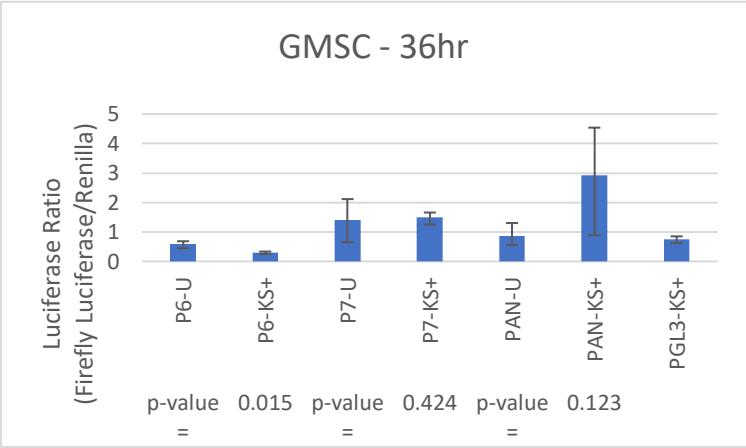

c.

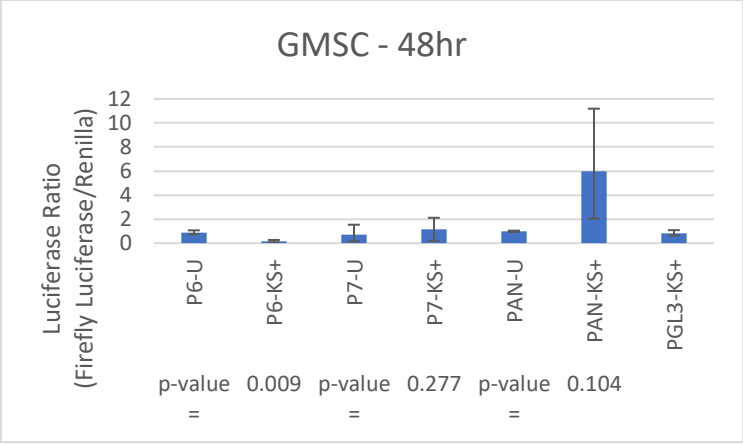

Figure 20: a. GMSC transfected with pGL3-pPROX1 v7 when infected with KSHV did show an increase in luciferase activity compared to its uninfected counterpart, but with a p-value of 0.072. **b.** pPAN in the KSHV+ sample showed an increase in luciferase signal but with high variability across samples, as shown by a wide error bar range. **c.** pPAN in the KSHV+ sample showed an increase in luciferase signal while all other samples are nearly identical to the pPGL3 empty vector control.

Chapter 4

Discussion:

In this experiment two overlapping versions of the PROX1 promoter (version 6 and version 7) were cloned into the luciferase reporting vector pGL3. Due to technical constraints, promoters were cloned first into an intermediary vector pCR2.1 using TA cloning, after each successful clone using either pGL3 or pCR2.1. Through restriction enzyme digest and gel electrophoresis the transformants were confirmed, followed by sequencing.

A method was established to calculate a viral titer in purified KSHV samples prior to infection. Previous equipment in the Yuan lab was replaced by a new Thermo Fisher Applied BioSystems Quantstudio 3 Real-Time PCR System, and therefore a new methodology was required prior to continuing with experiments. In order to infect cultures at 50 MOI using a standardized volume, we successfully were able to determine our viroid concentration to be 2.5x10^6 viral particles/ and visually confirmed infection through immunofluorescence microscopy using the GFP reporter under the KSHV PAN promoter, which has been previously integrated into our lab's KSHV genome.

Working with mesenchymal stem cells is a new set of techniques for the Yuan lab and we have shown that transfection using Lipofectamine 3000 with P3000 reagent resulted with the least cytotoxic lipofectamine reagent. Further work into determining a less cytotoxic method with higher transfection rates will continue to be worked on while our

lab continues to work with MSCs into the future. For example, Promega FuGENE or a lentivirus infection method may be a better approach and should be vetted in future attempts. Regardless, we have shown that KSHV infected 293T when transfected with pGL3-pPAN shows an increase in luciferase signal compared to the uninfected control. We were unable to consistently show an increase in the luciferase ratio using pGL3-pPAN in uninfected versus KSHV infected PDLSCs and GMSCs. Furthermore, both PDLSCs, GMSCs, and 293T cells do not show a noticeable change in luciferase signal using both version 6 and version 7 of the PROX1 promoter when infected with KSHV.

Future directions:

The future directions for this project has many potential routes. Firstly, we should reassess our initial observations regarding the upregulation of PROX1 in mesenchymal cells following KSHV infection. We should assess for upregulation via Western Blot and RT-PCR. Assessing for Prox1 protein would require acquiring either a commercially available Prox1 antibody or purification of Prox1 for the entire process of creating a usable specific antibody, including steps of immunogen preparation, immunization, hybridoma creation, collection, screening, isotyping, and purification through a commercial firm. As for the RT-PCR assay, this would require us to acquire PROX1 specific primers that span an exon-exon junction to reduce false detection from genomic DNA rather than the cDNA from the biological sample.

Further work needs to be done in identifying the PROX1 promoter sequence as well. There is very little literature regarding the promoter sequence and annotations on public

databases for the promoter region is limited and heavily reliant on computational models.

First a system where we can test and dissect the promoter using promoter: reporter fusions should and could be established. Next we should establish that the full length promoter is active. We could perform a 5' prime deletion series until activity is lost. This loss of function approach will identify the smallest region of the promoter that is necessary to induce gene expression. A gain of function assay using a limited library of synthetic PROX1 promoters that we have identified as the functional areas of the promoter should then be performed to prove biological activity, rather than implied computation evidence.

Future work will also focus on the role of Prox1 in KSHV infected mesenchymal cells. A knock-down experiment of using a lentiviral shRNA approach and a separate over-expression assay using the PROX1 CDS under an always-on promoter, or even the KSHV PAN promoter, followed by RNA-seq in KSHV infected and non-infected MSC samples would be a boon of valuable insight into the role of PROX1.

Furthermore, identifying PROX1 as a therapeutic target could be done through over-expression and/or knock-down of PROX1 in MSC-KSHV infected cell samples followed by renal capsule xenografting or subcutaneous pellet implantation in a murine model to evaluate a change in tumorigenesis. We would expect the knock-down of PROX1 to

reduce tumorigenesis while the upregulation of PROX1 to actually increase the rate of tumorigenesis given our current model and understanding.

In conclusion, KS is undeniably the most common malignancy HIV patients suffer from. It is characterized by abnormal inflammation neoagniogensis and proliferation of spindle cells[4,5,29]. Examining the cellular origin of KS and the method in which the tumor affects the normal differential pathways through specific transcriptional factors like PROX1 is crucial to understanding the diseases progression.

References:

1. Elsir T, Smits A, Lindstrom MS, Nister M. Transcription Factor PROX1: its Role in Development and Cancer. Cancer Metastasis Reviews 2012;31:793-805.
2. Groger M, Loewe R, Holnthoner W, et al. IL-3 Induces Expression of Lymphatic Markers PROX-1 and Podoplanin in Human Endothelial Cells. Journal of Immunology (Baltimore, Md : 1950) 2004;173:7161-9.
3. Li Y, Zhong C, Liu D, et al. Evidence for Kaposi's Sarcoma Originating from Mesenchymal Stem Cell through KSHV-induced Mesenchymal-to-Endothelial Transition. Cancer Res 2017.
4. Radu O, Pantanowitz L. Kaposi Sarcoma. Archives of Pathology & Laboratory Medicine 2013;137:289-94.
5. Antman K, Chang Y. Kaposi's Sarcoma. New England Journal of Medicine 2000;342:1027-38.
6. Ganem D. KSHV infection and the Pathogenesis of Kaposi's Sarcoma. Annu Rev Pathol Mech Dis 2006;1:273-96.
7. Ganem D. KSHV and the Pathogenesis of Kaposi Sarcoma: Listening to Human Biology and Medicine. The Journal of Clinical Investigation 2010;120:939-49.
8. Cancian L, Hansen A, Boshoff C. Cellular Origin of Kaposi's Sarcoma and Kaposi's Sarcoma-Associated Herpesvirus-Induced Cell Reprogramming. Trends in Cell Biology 2013;23:421-32.
9. Gurzu S, Ciortea D, Munteanu T, Kezdi-Zaharia I, Jung I. Mesenchymal-to-endothelial transition in Kaposi Sarcoma: a Histogenetic Hypothesis Based on a Case Series and Literature Review. PloS one 2013;8:e71530.
10. Cancian L, Hansen A, Boshoff C. Cellular Origin of Kaposi's Sarcoma and Kaposi's Sarcoma-associated Herpesvirus-Induced Cell Reprogramming. Trends in Cell Biology 2013;23:421-32.
11. Abe Y, Matsubara D, Gatanaga H, et al. Distinct Expression of Kaposi's Sarcoma-Associated Herpesvirus-encoded proteins in Kaposi's Sarcoma and Multicentric Castleman's Disease. Pathology International 2006;56:617-24.
12. Renne R, Barry C, Dittmer D, Compitello N, Brown PO, Ganem D. Modulation of Cellular and Viral Gene Expression by the Latency-Associated Nuclear Antigen of Kaposi's Sarcoma-Associated Herpesvirus. Journal of Virology 2001;75:458-68.
13. Johnson NC, Dillard ME, Baluk P, et al. Lymphatic Endothelial Cell Identity is Reversible and its Maintenance Requires PROX1 Activity. Genes & Development 2008;22:3282-91.
14. Benevenuto de Andrade BA, Ramírez-Amador V, Anaya-Saavedra G, et al. Expression of PROX-1 in Oral Kaposi's Sarcoma Spindle Cells. Journal of Oral Pathology & Medicine 2014;43:132-6.
15. Li Y, Zhong C, Liu D, et al. Evidence for Kaposi Sarcoma Originating from Mesenchymal Stem Cell through KSHV-induced Mesenchymal-to-Endothelial Transition. Cancer Research 2018;78:230-45.
16. Takahashi M, Yoshimoto T, Shimoda M, et al. Loss of Function of the Candidate Tumor Suppressor PROX1 by RNA Mutation in Human Cancer Cells. Neoplasia 2006;8:1003-10.

17. Dadras SS, Skrzypek A, Nguyen L, et al. PROX-1 Promotes Invasion of Kaposiform Hemangioendotheliomas. Journal of Investigative Dermatology 2008;128:2798-806.
18. Lavado A, Oliver G. PROX1 Expression Patterns in the Developing and Adult Murine Brain. Developmental Dynamics 2007;236:518-24.
19. Hong YK, Harvey N, Noh YH, et al. PROX1 is a Master Control Gene in the Program Specifying Lymphatic Endothelial Cell Fate. Developmental Dynamics : an official publication of the American Association of Anatomists 2002;225:351-7.
20. Duverger O, Morasso MI. Role of Homeobox Genes in the Patterning, Specification and Differentiation of Ectodermal Appendages in mammals. Journal of Cellular Physiology 2008;216:337-46.
21. Hong YK, Harvey N, Noh YH, et al. PROX1 is a Master Control Gene in the Program Specifying Lymphatic Endothelial Cell Fate. Developmental Dynamics 2002;225:351-7.
22. Elsir T, Smits A, Lindström MS, Nistér M. Transcription Factor PROX1: its Role in Development and Cancer. Cancer and Metastasis Reviews 2012;31:793-805.
23. Rodrigues MF, de Oliveira Rodini C, de Aquino Xavier FC, et al. PROX1 Gene is Differentially Expressed in Oral Cancer and Reduces Cellular Proliferation. Medicine 2014;93:e192.
24. Yoo J, Kang J, Lee HN, et al. Kaposin-B Enhances the PROX1 mRNA Stability During Lymphatic Reprogramming of Vascular Endothelial Cells by Kaposi's Sarcoma Herpes virus. PLoS Pathog 2010;6:e1001046.
25. Brulois KF, Chang H, Lee AS, et al. Construction and Manipulation of a New Kaposi's Sarcoma-Associated Herpesvirus Bacterial Artificial Chromosome Clone. J Virol 2012;86:9708-20.
26. Zhou B, Si W, Su Z, Deng W, Tu X, Wang Q. Transcriptional Activation of the PROX1 Gene by HIF-1α and HIF-2α in Response to Hypoxia. FEBS letters 2013;587:724-31.
27. de Carvalho TG, Pellenz FM, Laureano A, et al. A simple protocol for Transfecting Human Mesenchymal Stem Cells. Biotechnology Letters 2018;40:617-22.
28. Campbell M, Watanabe T, Nakano K, et al. KSHV Episomes Reveal Dynamic Chromatin Loop Formation with Domain-Specific Gene Regulation. Nature Communications 2018;9:49.
29. Dourmishev LA, Dourmishev AL, Palmeri D, Schwartz RA, Lukac DM. Molecular Genetics of Kaposi's Sarcoma-Associated Herpesvirus (Human Herpesvirus-8) Epidemiology and Pathogenesis. Microbiology and Molecular Biology Reviews : MMBR 2003;67:175-212, table of contents.